Protein Stability, Folding and Dynamics

CHEM 420 – Principles of Biochemistry
Instructor – Anthony S. Serianni

Chapters 8 and 9: Voet/Voet, *Biochemistry*, 2011
Fall 2015

September 21 & 23

Graphical
Representation
and Analysis of
Surface
Properties

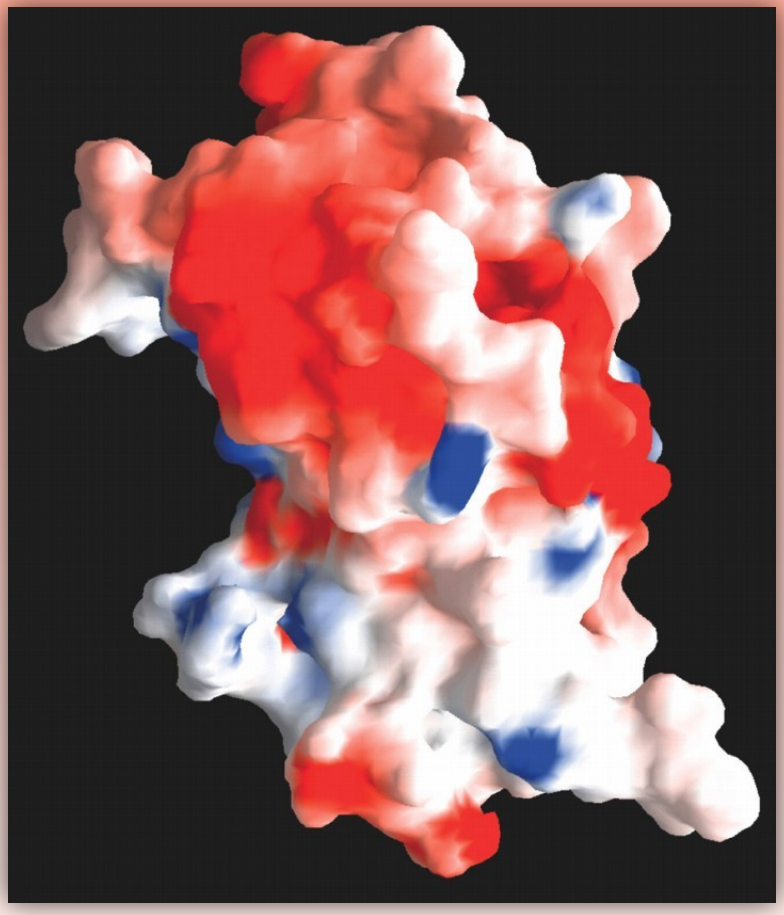

red = (-)
blue = (+)
white = neutral

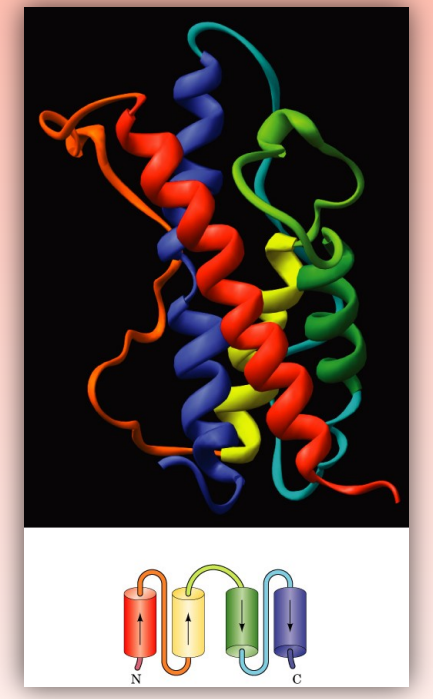

A GRASP diagram of human growth hormone
(helps predict protein interactions with charged molecules)

Protein Structure Prediction

Secondary structure
(A) Chou-Fasman method

Frequency at which a given amino acid occurs in an α helix in a set of protein structures $= f_\alpha = n_\alpha/n$, where n_α = number of amino acid residues of the given type (e.g., alanine) that occur in α helices, and n = total number of residues of this type (i.e., total alanines) in the protein set.

Propensity of a particular amino acid residue to occur in an α helix = $P_\alpha = f_\alpha/\langle f_\alpha \rangle$, where $\langle f_\alpha \rangle$ is the average value of f_α for all 20 residues.

When $P_\alpha > 1$: residue occurs with greater than average frequency in an α helix

Also applies to β-structure

Residue	P_α	Helix Classification	P_β	Sheet
Ala	1.42	H_α	0.83	i_β
Arg	0.98	i_α	0.93	i_β
Asn	0.67	b_α	0.89	i_β
Asp	1.01	I_α	0.54	B_β
Cys	0.70	i_α	1.19	h_β
Gln	1.11	h_α	1.10	h_β
Glu	1.51	H_α	0.37	B_β
Gly	0.57	B_α	0.75	b_β
His	1.00	I_α	0.87	h_β
Ile	1.08	h_α	1.60	H_β
Leu	1.21	H_α	1.30	h_β
Lys	1.16	h_α	0.74	b_β
Met	1.45	H_α	1.05	h_β
Phe	1.13	h_α	1.38	h_β
Pro	0.57	B_α	0.55	B_β
Ser	0.77	i_α	0.75	b_β
Thr	0.83	i_α	1.19	h_β
Trp	1.08	h_α	1.37	h_β
Tyr	0.69	b_α	1.47	H_β
Val	1.06	h_α	1.70	H_β

Source: Chou, P.Y. and Fasman, G.D., *Annu. Rev. Biochem.* **47,** 258 (1978).

H = strong former
h = former
I = weak former
i = indifferent
b = breaker
B = strong breaker

Propensities and classifications of amino acid residues for α helical and β sheet conformations

(B) Reverse turns: Rose method

Occur on the surface of a protein; occur at positions along the polypeptide chain where the hydropathy is a minimum (exclude helical regions)

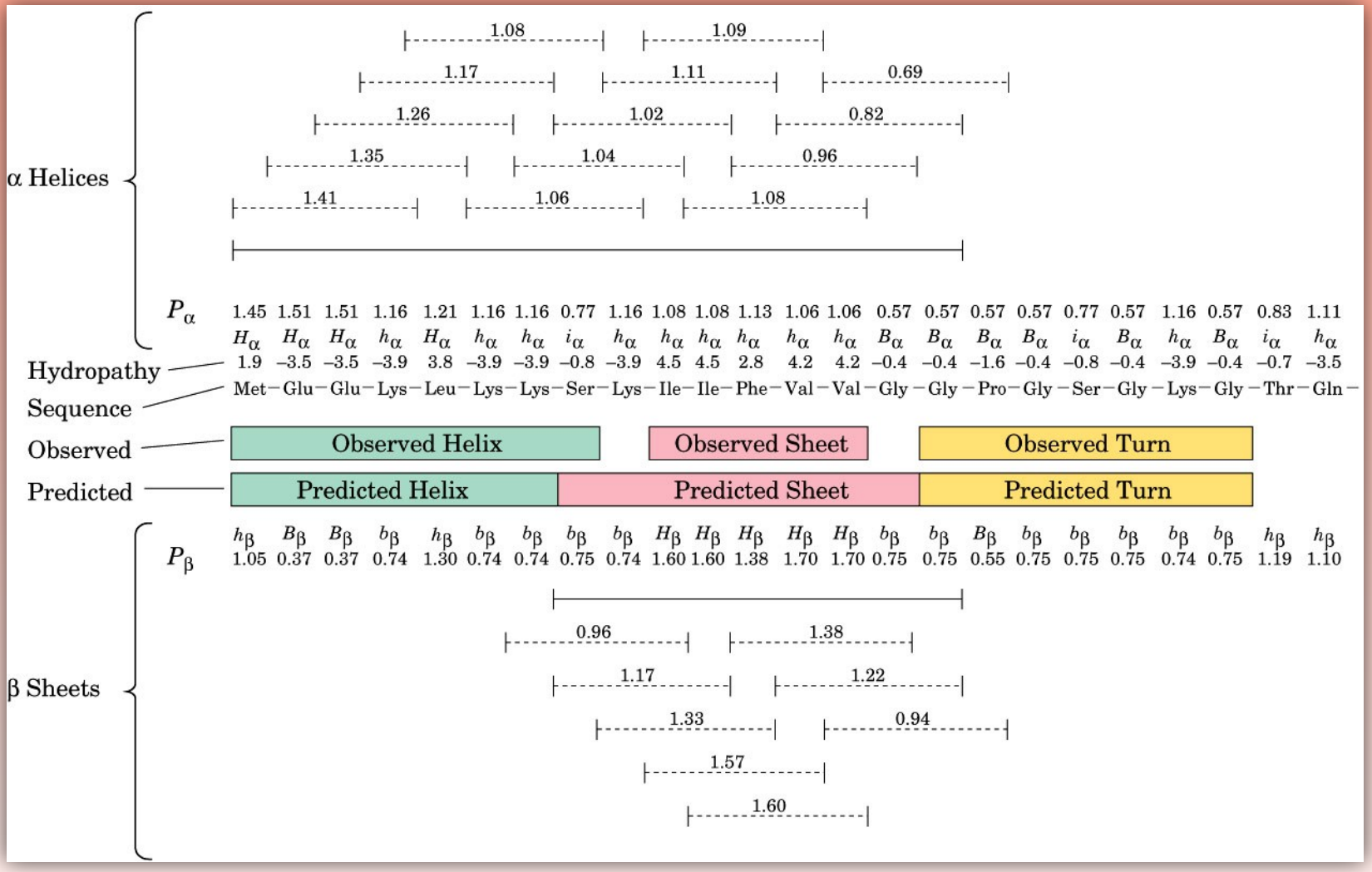

Secondary structure prediction in adenylate kinase
(*N*-terminal 24 residues)

Values become increasingly negative as the side chain increases in hydrophilicity

Side Chain	Hydropathy	
Ile	4.5	
Val	4.2	
Leu	3.8	
Phe	2.8	
Cys	2.5	
Met	1.9	
Ala	1.8	
Gly	0.4	
Thr	0.7	
Ser	0.8	
Trp	0.9	
Tyr	1.3	
Pro	1.6	negative in sign
His	3.2	
Glu	3.5	
Gln	3.5	
Asp	3.5	
Asn	3.5	
Lys	3.9	
Arg	4.5	

Source: Kyte, J. and Doolitle, R.F., *J. Mol. Biol.* **157,** 110 (1982).

Hydropathy scale for amino acid side chains

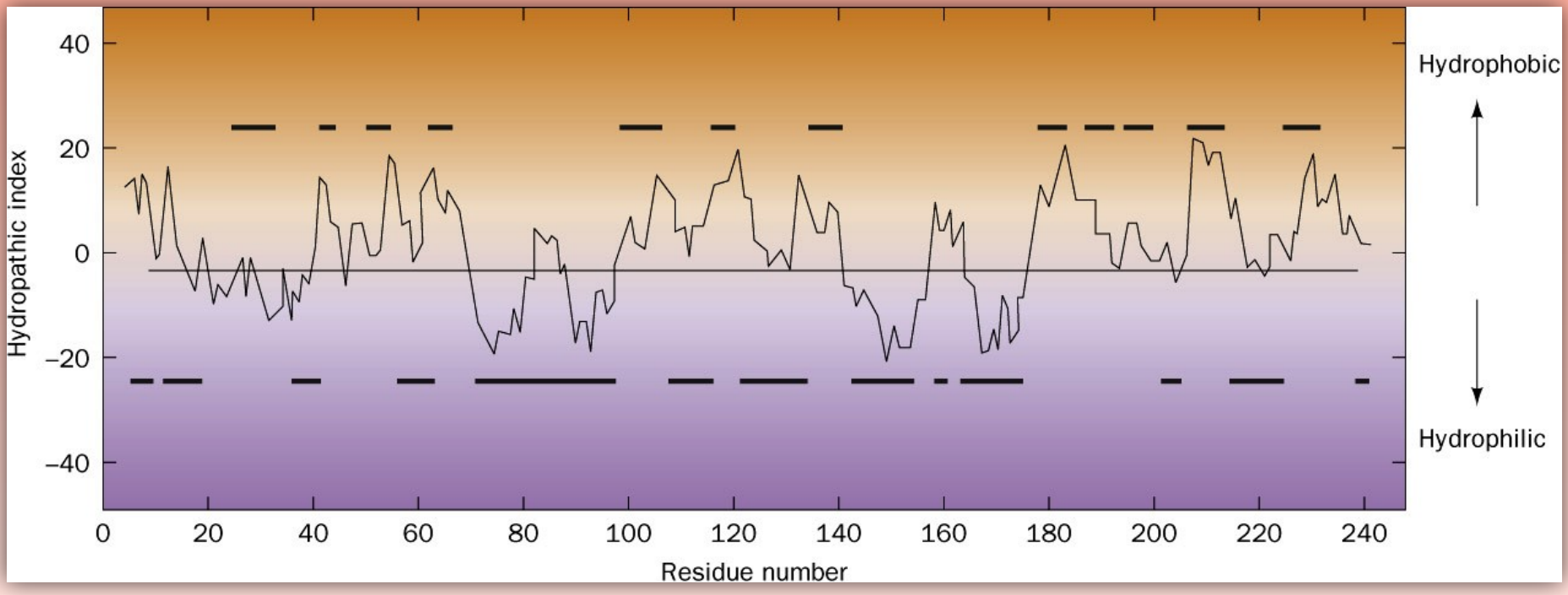

Hydropathic index plot for bovine chymotrypsinogen. Bars indicate exterior (below) and interior (above) regions of the protein, determined by crystallography.

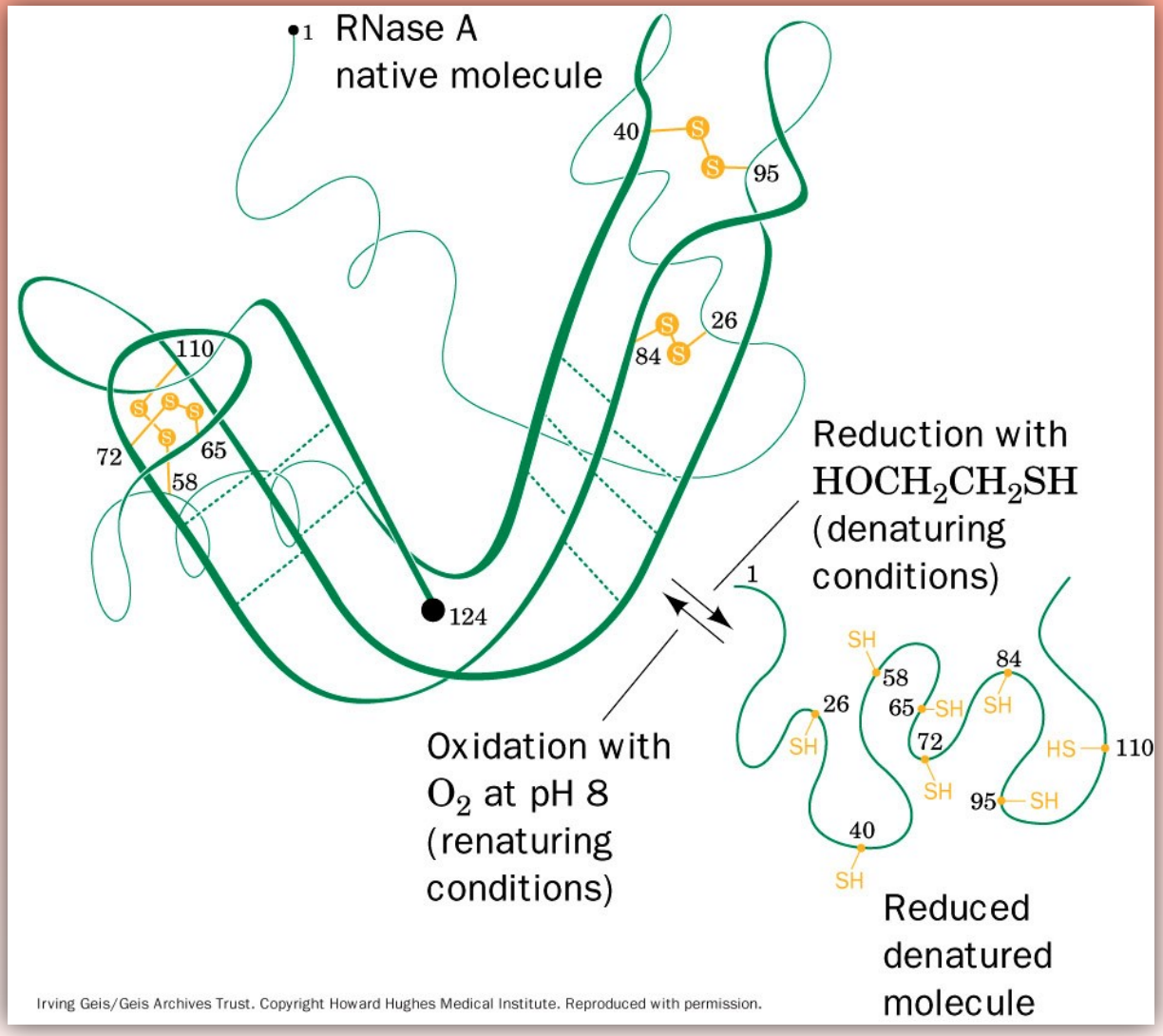

Reductive denaturation and oxidative renaturation of RNase A

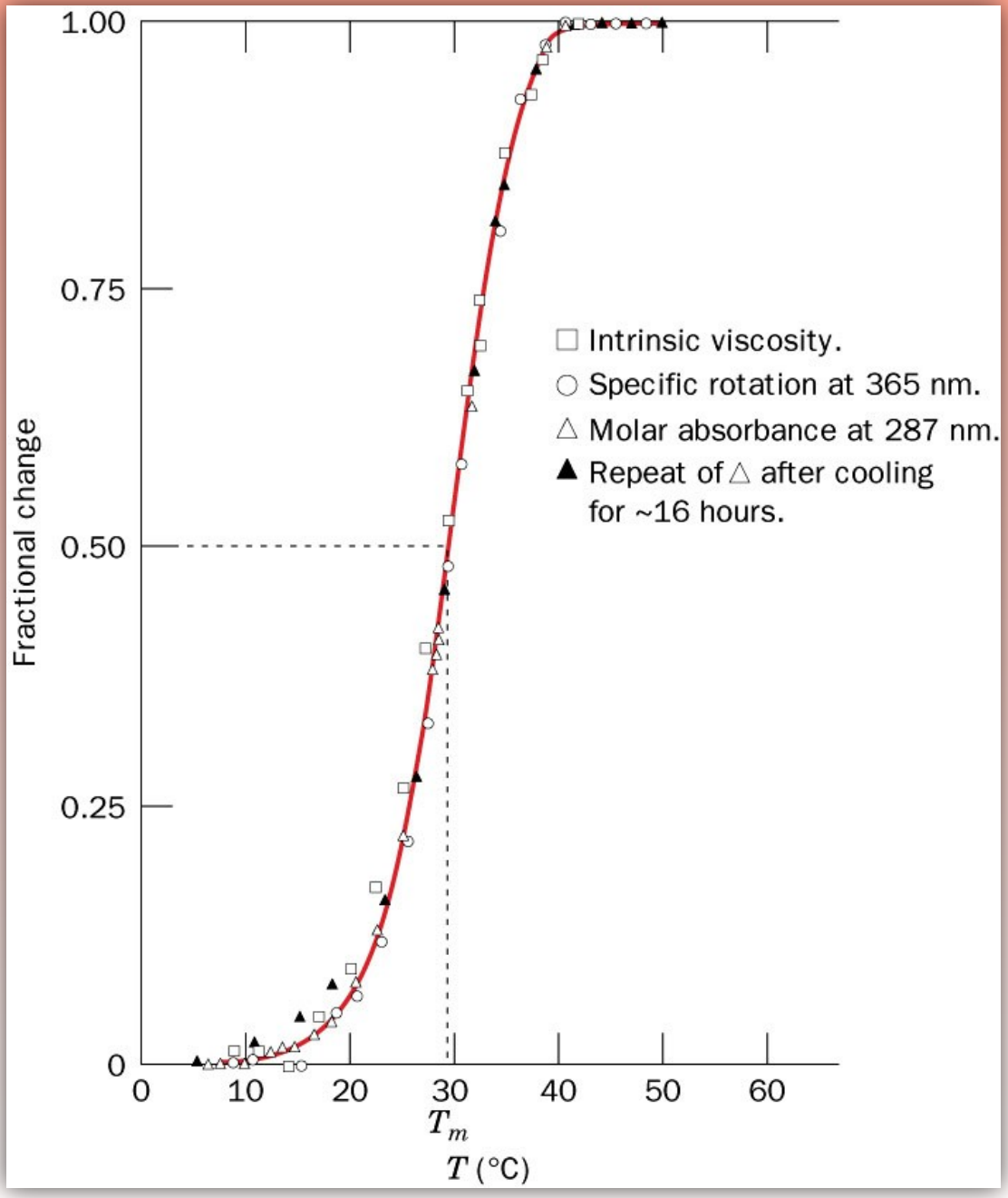

Heat-induced protein denaturation curve: RNase A (cooperative unfolding)

Denatured RNase renatures upon cooling; renaturation is not observed for many proteins.

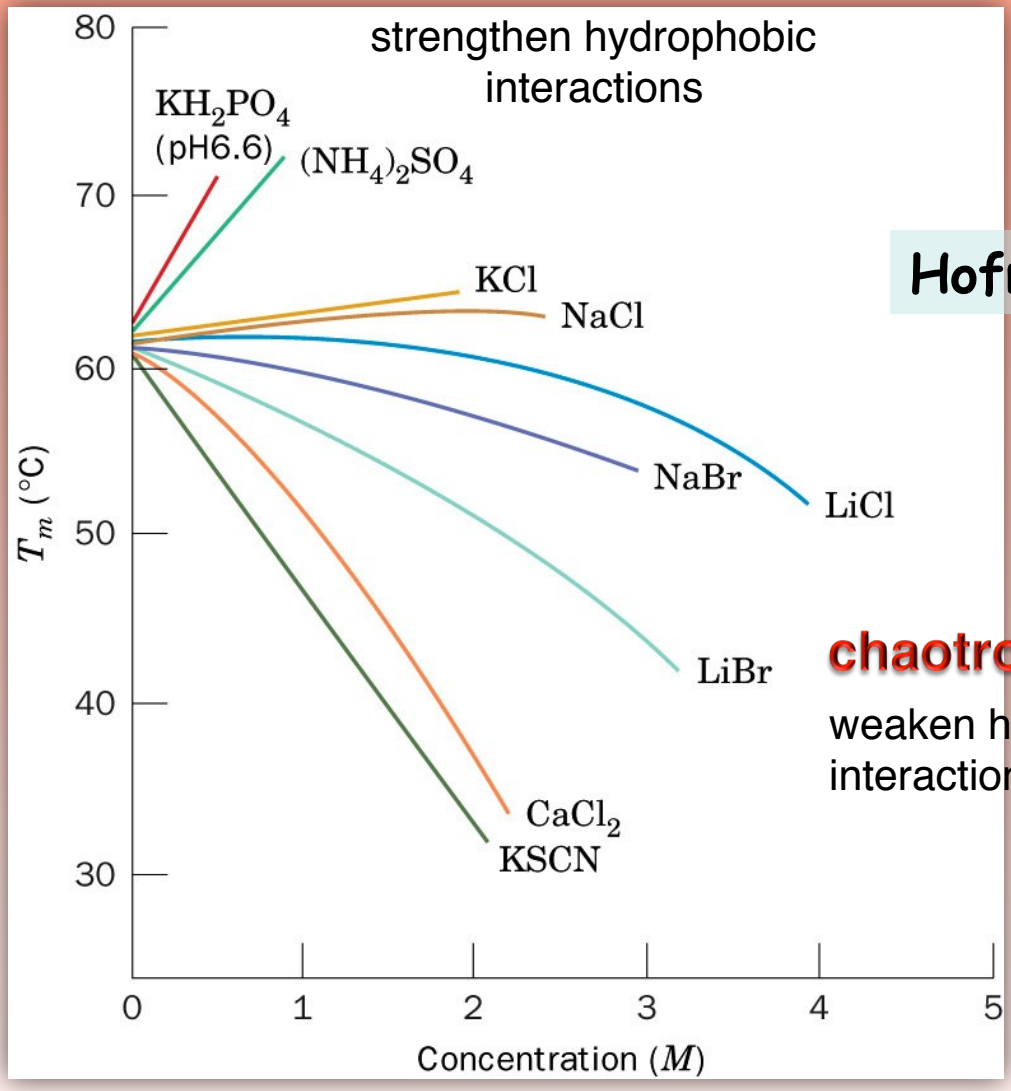

Hofmeister series

chaotropic salts

weaken hydrophobic interactions

Melting temperature of RNase A as a function of the concentration of various salts

Some determinants of protein folding

A. Helices/sheets predominate in proteins because they fill space efficiently.

B. Protein folding is directed mainly by internal residues (protein folding is driven by hydrophobic forces – the *hydrophobic* effect).

C. Protein fold depends on primary sequence.

Process	ΔH (kJ · mol^{-1})	$T\Delta S_u$ (kJ · mol^{-1})	ΔG_u -(kJ · mol^{-1})
CH_4 in $H_2O \rightleftharpoons$ CH_4 in C_6H_6	11.7	22.6	10.9
CH_4 in $H_2O \rightleftharpoons$ CH_4 in CCl_4	10.5	22.6	12.1
C_2H_6 in $H_2O \rightleftharpoons$ C_2H_6 in benzene	9.2	25.1	15.9
C_2H_4 in $H_2O \rightleftharpoons$ C_2H_4 in benzene	6.7	18.8	12.1
C_2H_2 in $H_2O \rightleftharpoons$ C_2H_2 in benzene	0.8	8.8	8.0
Benzene in $H_2O \rightleftharpoons$ liquid benzene[b]	0.0	17.2	17.2
Toluene in $H_2O \rightleftharpoons$ liquid toluene[b]	0.0	20.0	20.0

[a] ΔG_u, the **unitary Gibbs free energy change,** is the Gibbs free energy change, ΔG, corrected for its concentration dependence so that it reflects only the inherent properties of the substance in question and its interaction with solvent. This relationship, according to Equation [3.13], is

$$\Delta G_u = \Delta G - nRT \ln \frac{[A_f]}{[A_i]}$$

where $[A_i]$ and $[A_f]$ are the initial and final concentrations of the substance under consideration, respectively, and n is the number of moles of that substance. Since the second term in this equation is a purely entropic term (concentrating a substance increases its order), ΔS_u, the **unitary entropy change,** is expressed

$$\Delta S_u = \Delta S + nR \ln \frac{[A_f]}{[A_i]}$$

[b] Data measured at 18°C.

Source: Kauzmann, W., *Adv. Protein Chem.* **14,** 39 (1959).

Thermodynamic changes for transferring hydrocarbons from water to nonpolar solvents at 25°C; importance of the *hydrophobic effect* on protein folding

The Levinthal Paradox (1968): crude estimate of the time required for protein folding

For an *n*-residue protein with 2*n* backbone torsions (ϕ and ψ) and three stable conformations about each torsion: *~10^n total conformations*
If you explore 10^{13} conformations per second, then:

time to explore all potential conformations: $t = 10^n/10^{13}$ s

For a 100-residue protein: $t = 10^{87}$ s (> age of universe!)

Conclusion: proteins fold via an ordered pathway or set of pathways

Experimental methods to monitor protein folding in the laboratory

detection by
UV/VIS / fluorescence / CD

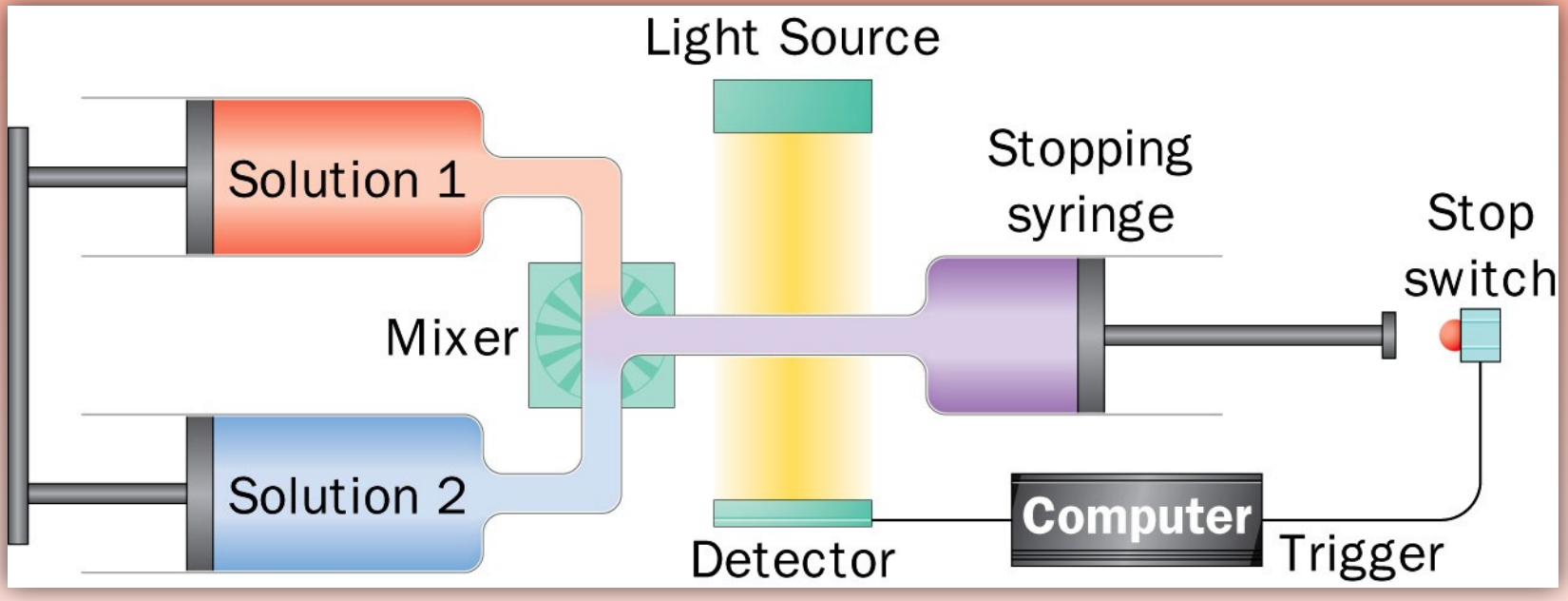

A stopped-flow device: 40 μs dead-times; reaction times are varied.

molar extinction coefficient

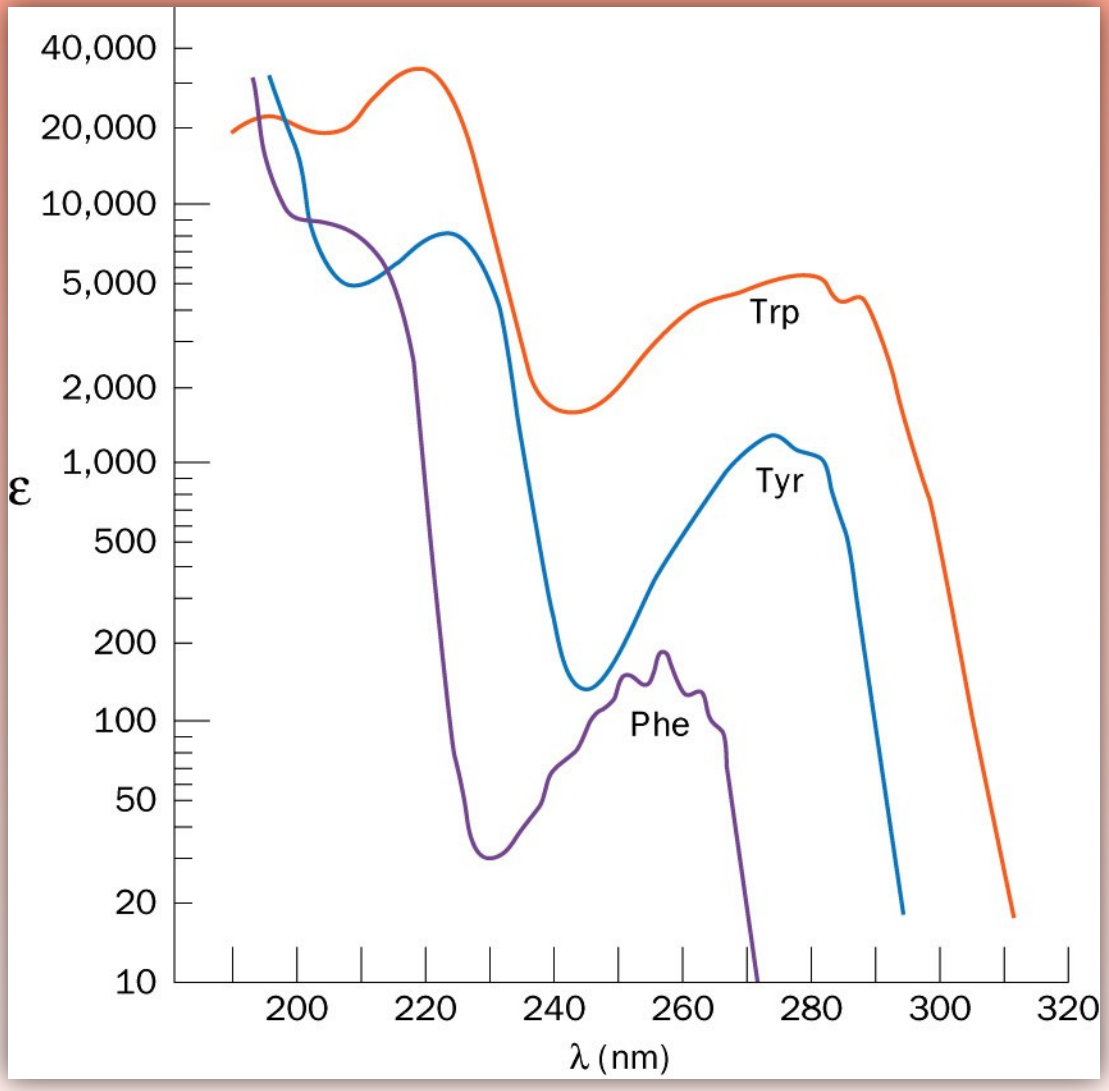

UV absorbance spectra of the three aromatic amino acids, phenylalanine, tryptophan, and tyrosine

Only chiral molecules give a CD spectrum.

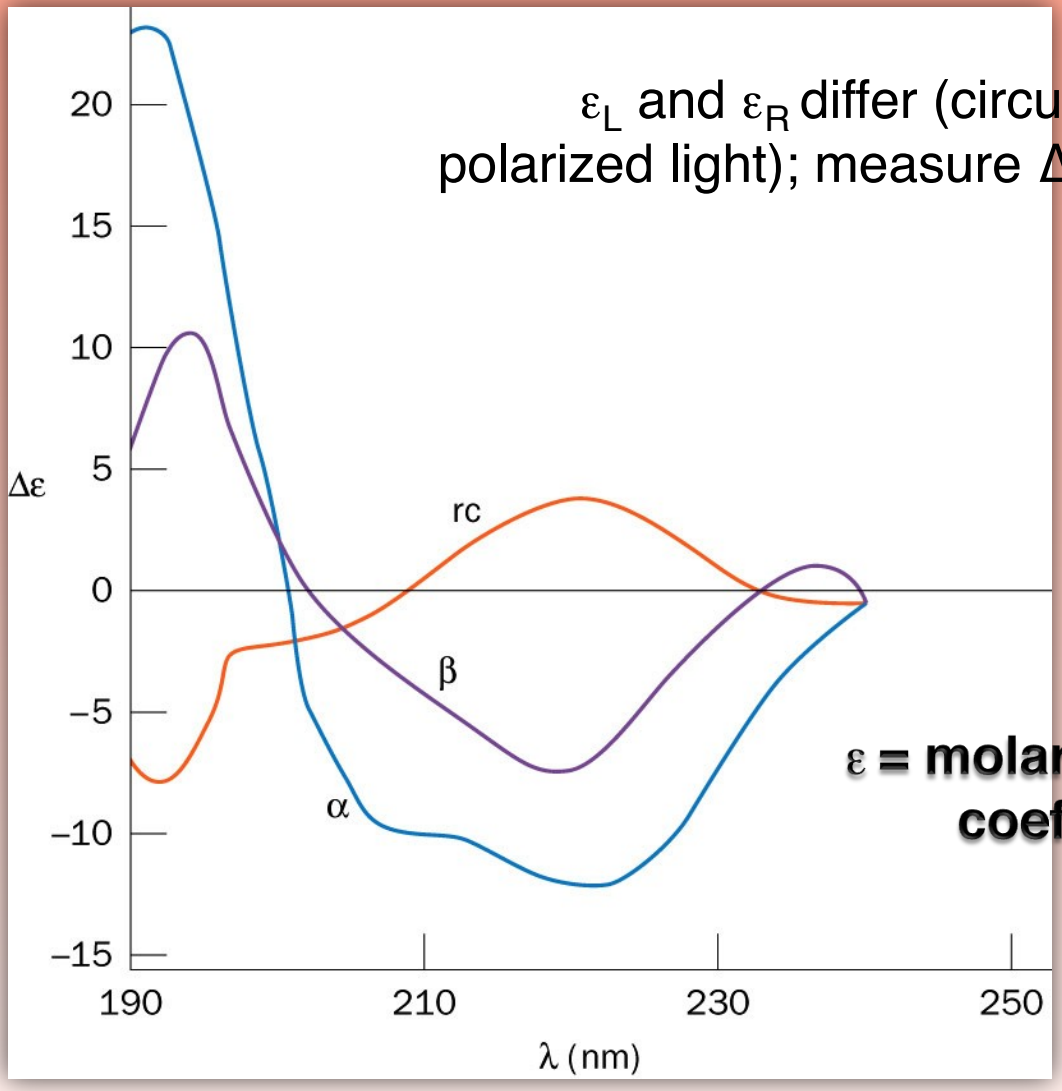

ε_L and ε_R differ (circularly polarized light); measure $\Delta\varepsilon = \varepsilon_L - \varepsilon_R$

ε = molar extinction coefficient

Circular dichroism (CD) spectra of polypeptides: α = α-helix; β = β-sheet; rc = random coil

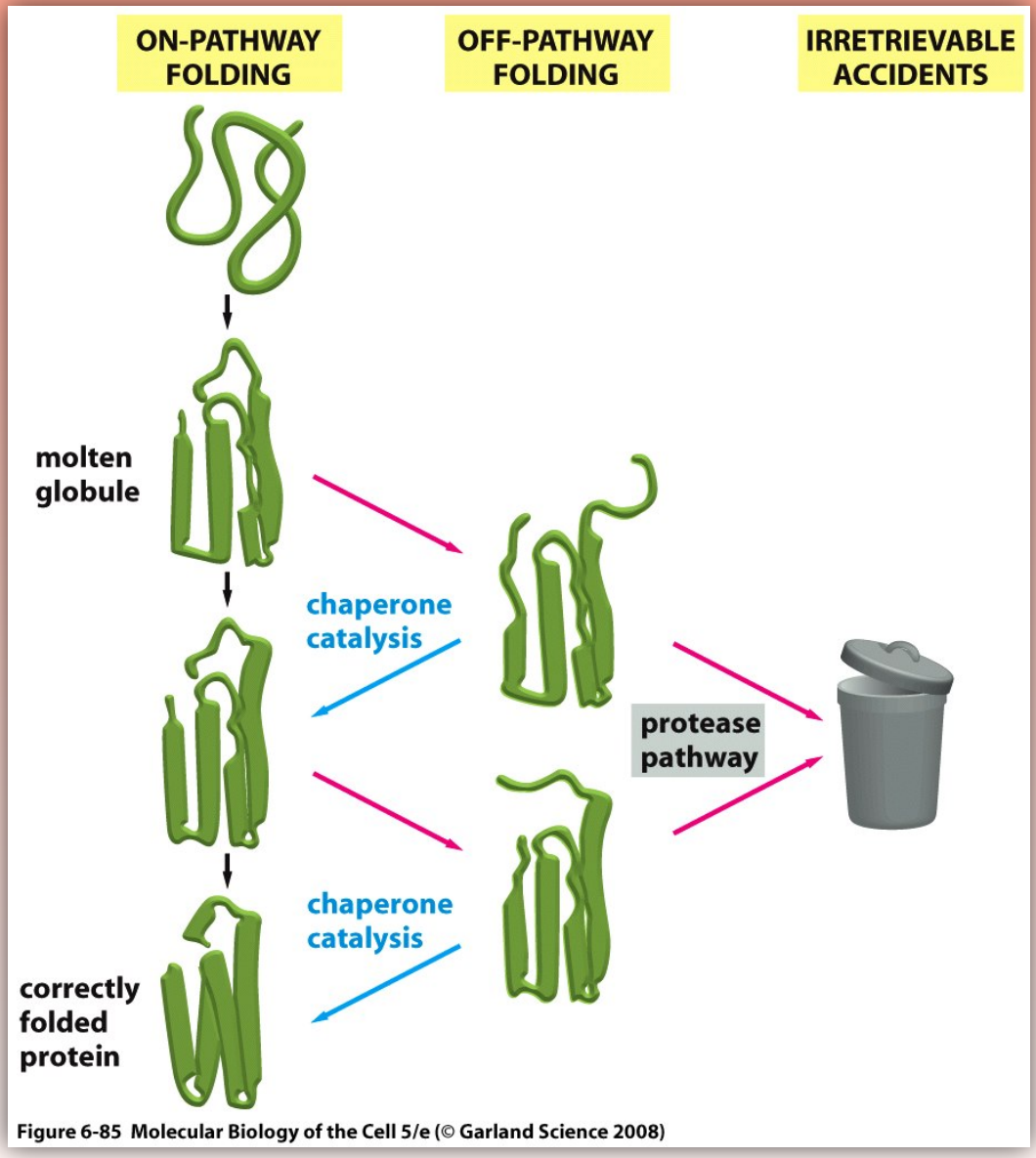

Figure 6-85 Molecular Biology of the Cell 5/e (© Garland Science 2008)

Overview of protein folding and degradation

Generalized Folding Pathway for Proteins

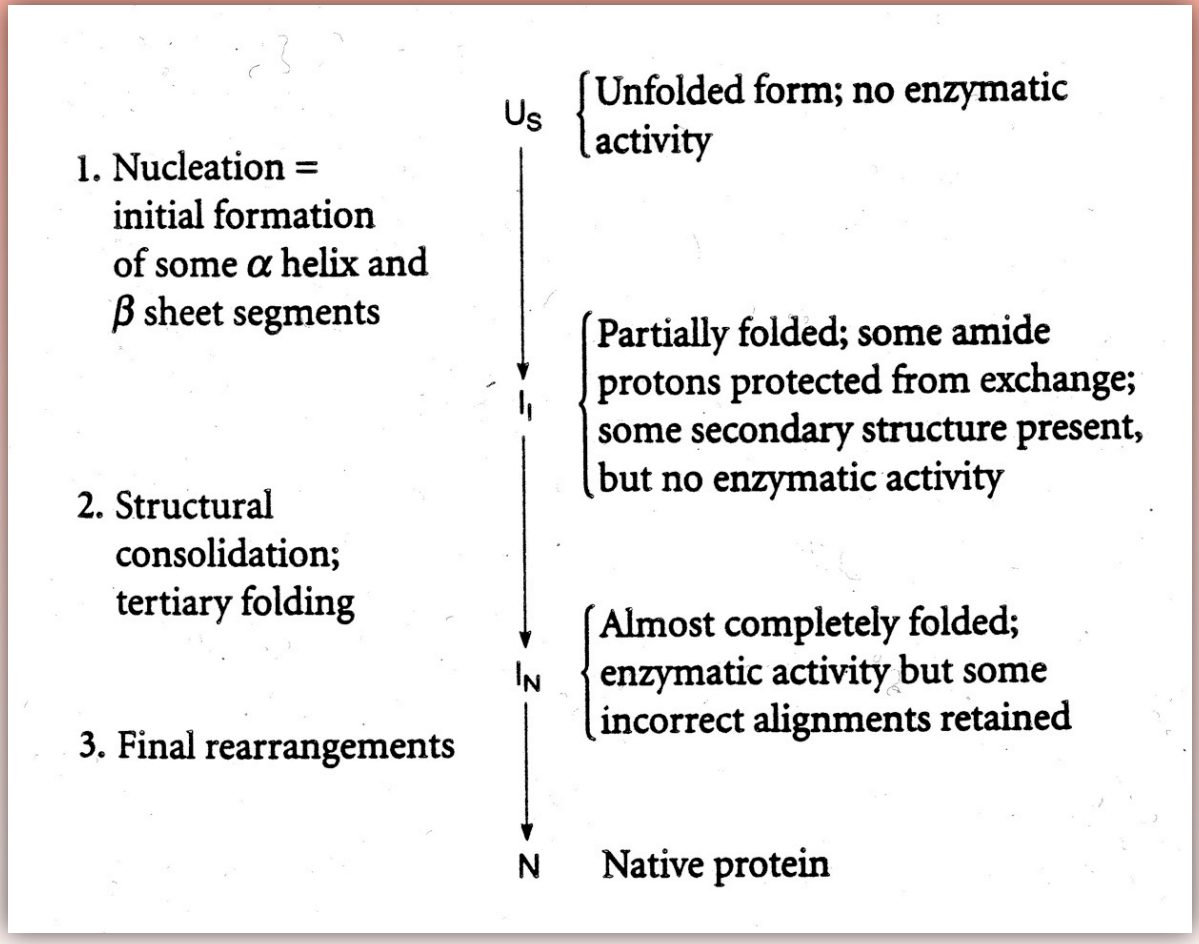

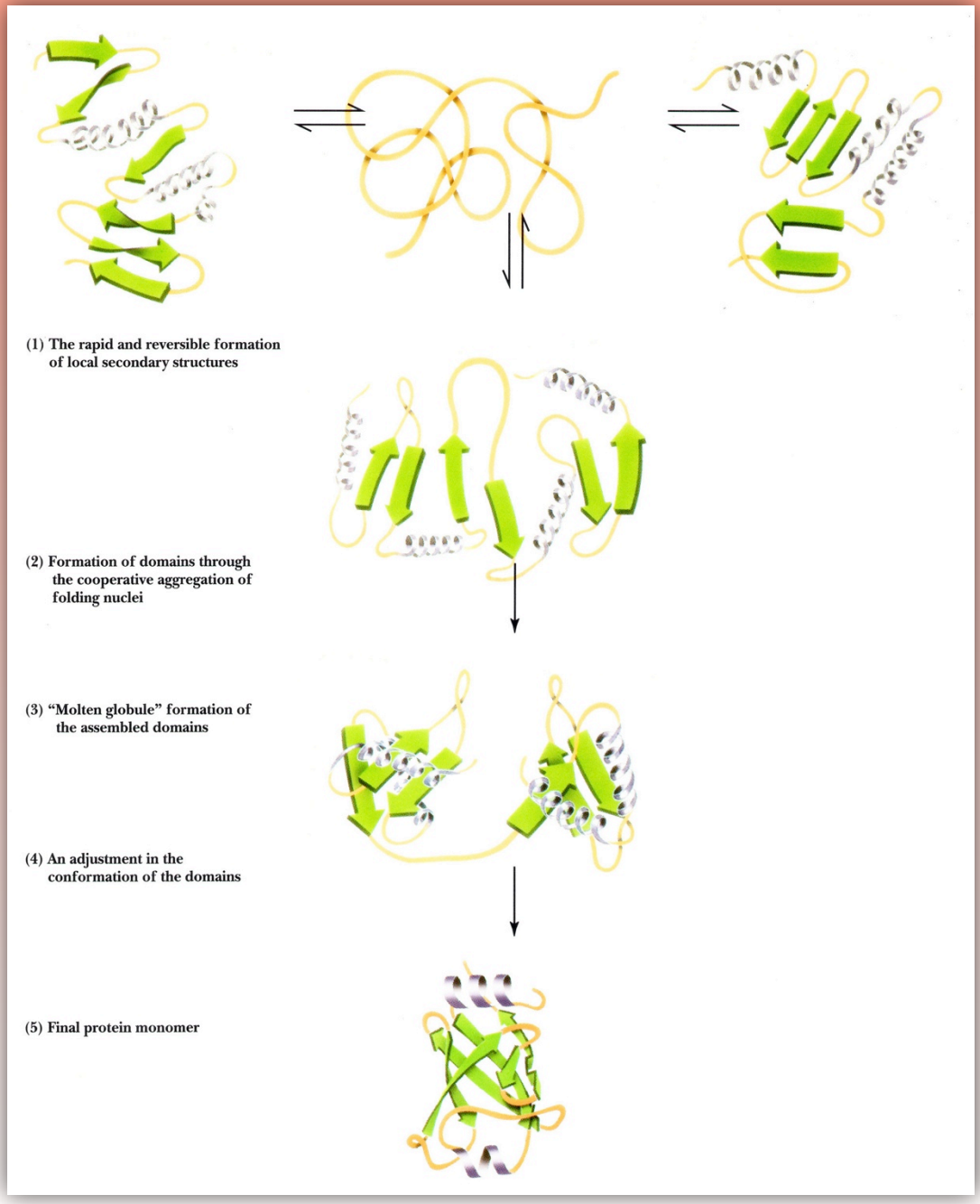

Roles of molten globule and domains in protein folding

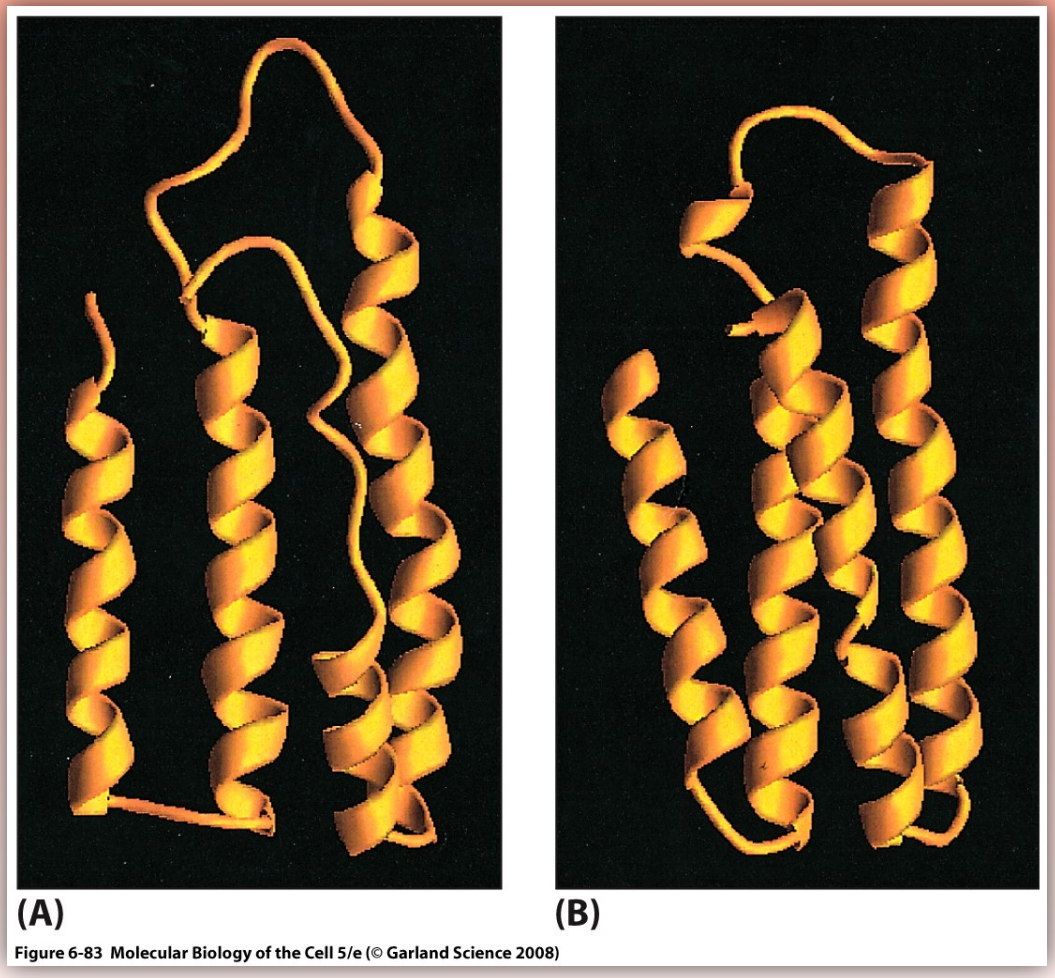

Figure 6-83 Molecular Biology of the Cell 5/e (© Garland Science 2008)

The structure of a molten globule. Cytochrome b_{562}. Molten globule structure (A) compared to the completely folded protein (B)

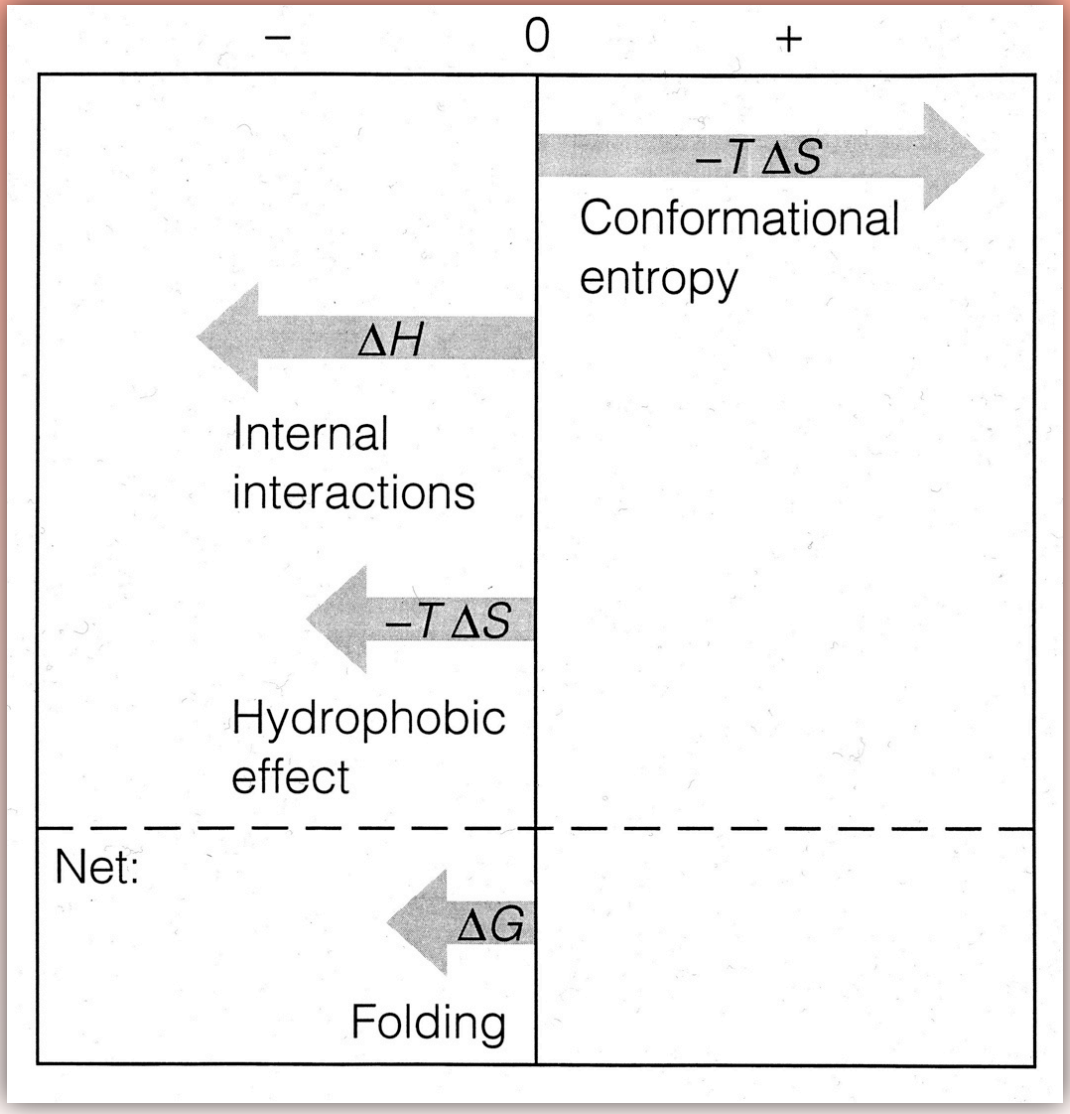

Competing physical forces that determine the free energy of protein folding

TABLE 6.3 Thermodynamic parameters for folding of some globular proteins at 25°C in aqueous solution

Protein	ΔG (kJ/mol)	ΔH (kJ/mol)	ΔS (J/°mol)
Ribonuclease	−46	−280	−790
Chymotrypsin	−55	−270	−720
Lysozyme	−62	−220	−530
Cytochrome *c*	−44	−52	−27
Myoglobin	−50	0	+170

Note: Data adapted from P. L. Privalov and N. N. Khechinashvili, *J. Mol. Biol.* (1974) 86:665–684. Each data set has been taken at the pH value where the protein is maximally stable; all are near physiological pH. Data are for the folding reaction: Denatured $\rightleftharpoons$ native.

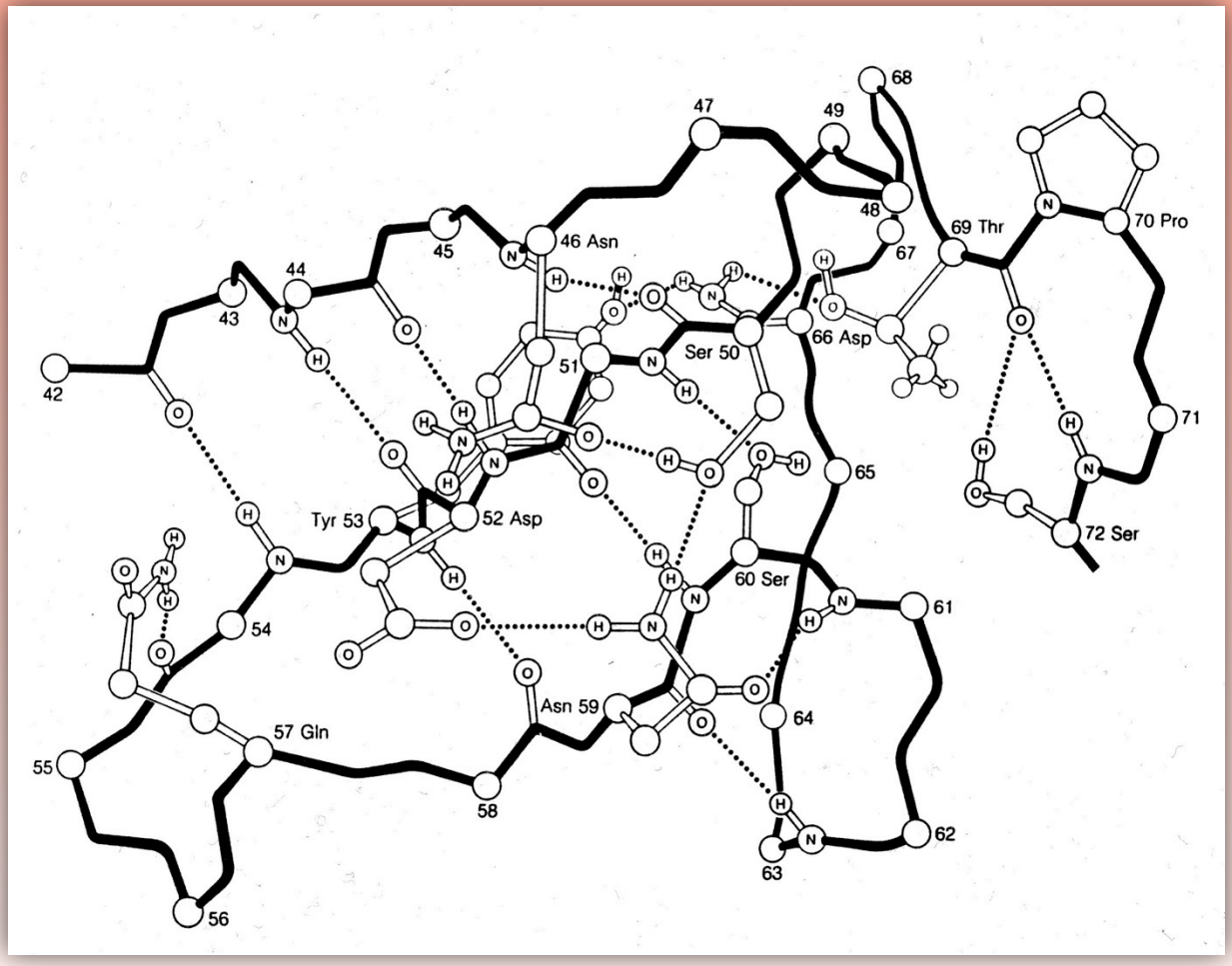

H-bonding patterns in a folded protein

Landscape Theory of Protein Folding

Polypeptides fold via a series of conformational adjustments that reduce their free energy and entropy until the native state is reached.

No single pathway or closely related set of pathways exist that a polypeptide must follow when folding to its native state.

Sequence information specifying a particular fold is distributed throughout the polypeptide chain and is highly over-determined.

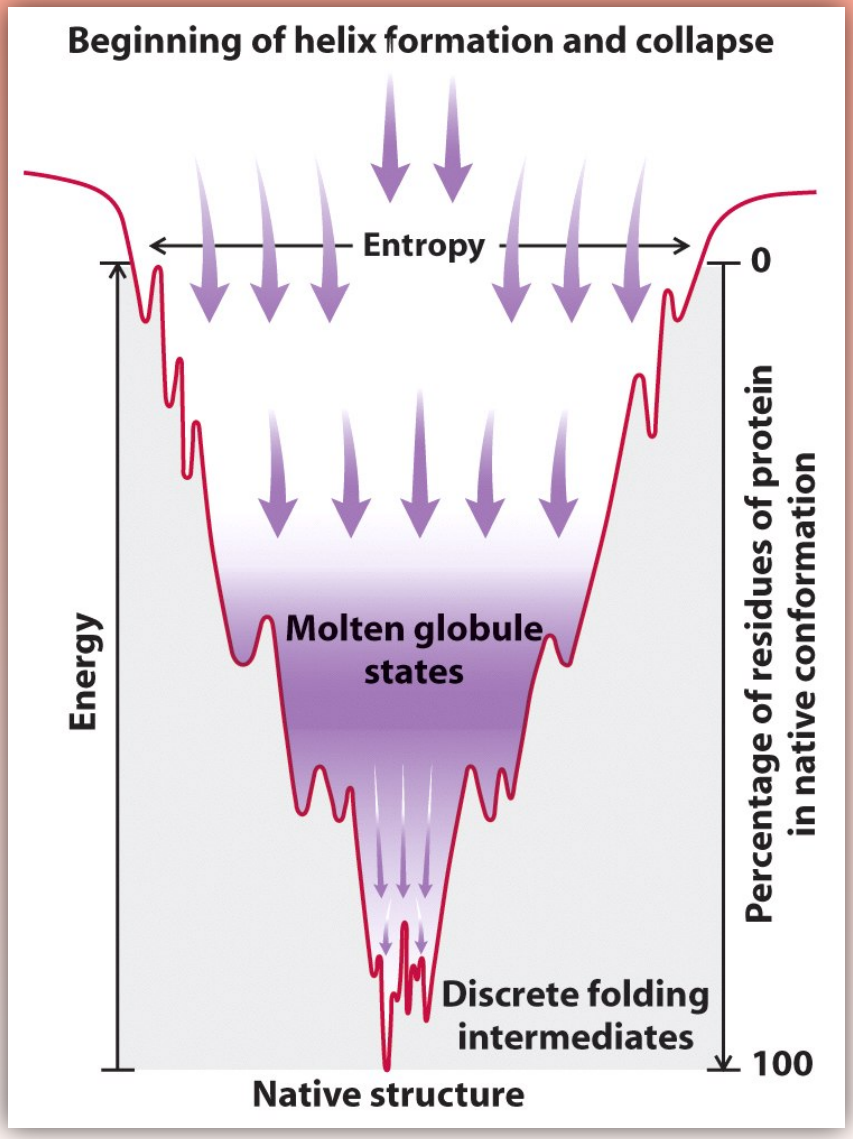

A 2D protein folding trajectory showing initiation, intermediates, and the native structure

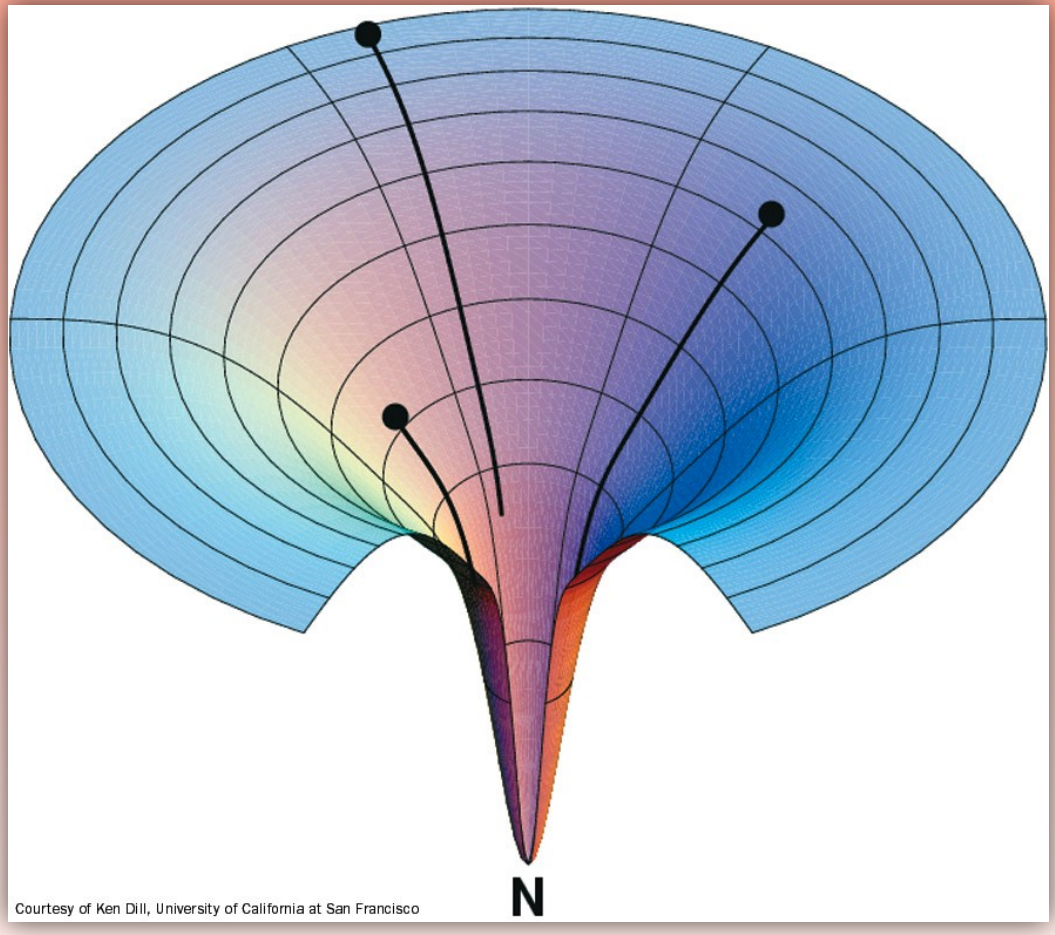

Courtesy of Ken Dill, University of California at San Francisco

Folding funnels: An idealized funnel landscape

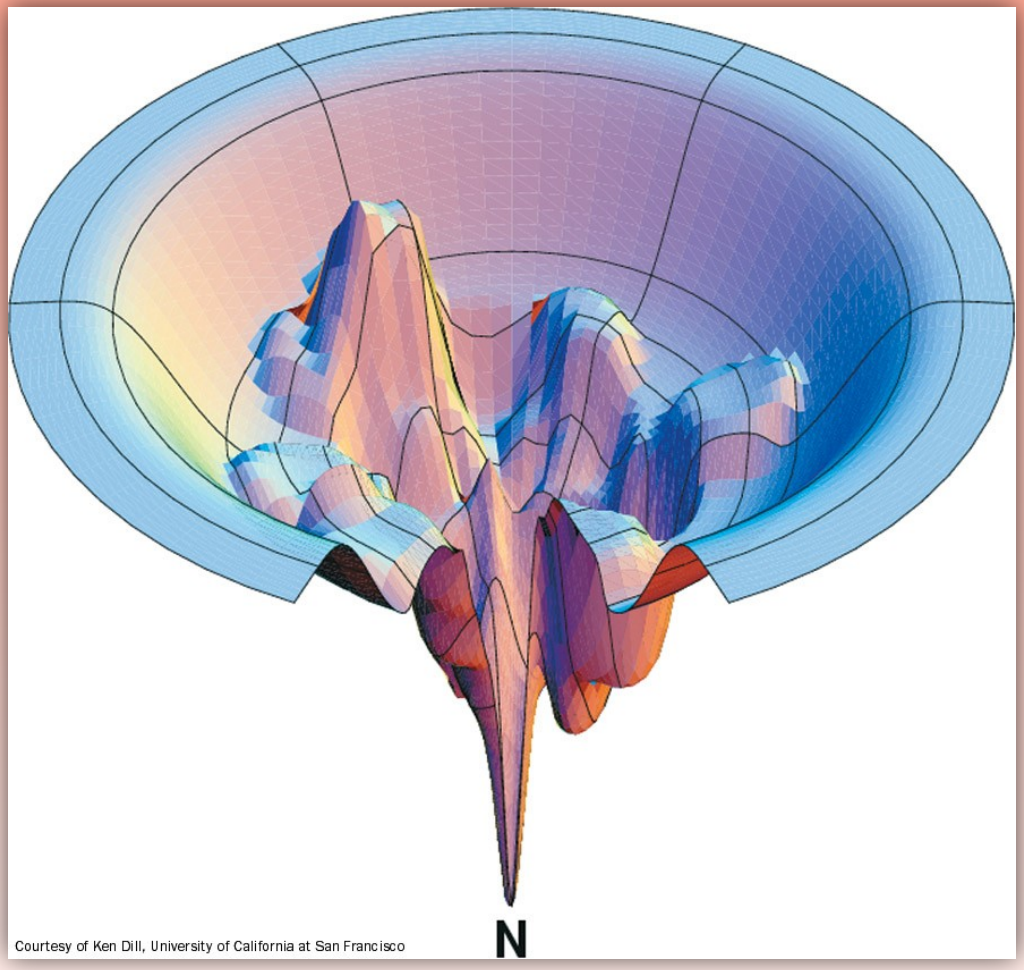

Courtesy of Ken Dill, University of California at San Francisco

Closer mimic of an actual folding pathway

Folding funnels: Rugged energy surface

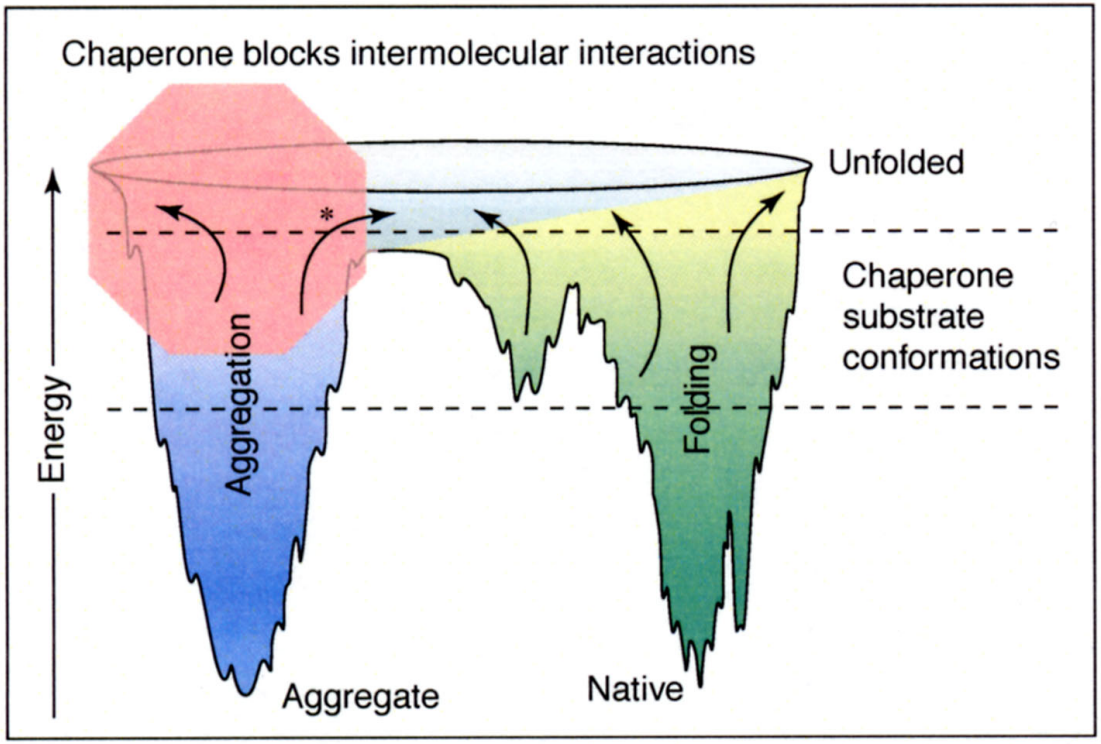

Figure 2. The effect of Hsp60 molecular chaperones on chain conformations in the context of a multiple-minima folding funnel. For simplicity, funnel space is shown only for stabilizing conformations. Hsp60 molecular chaperones recognize polypeptide chains (in either funnel) with conformations that expose significant amounts of hydrophobic surface area; these conformations are indicated by the area of the funnels within the broken lines. In the iterative annealing mechanism, the ATP hydrolysis cycle releases polypeptide chains with fewer stabilizing interactions or higher chain entropy (i.e. a higher position on the funnel surface, indicated by the curved black arrows), permitting a new path down the funnel surface that possibly traverses the barrier separating the folding and aggregation funnels (arrow marked with asterisk). In the Anfinsen cage mechanism [32], chain isolation in the central cavity of the chaperone effectively blocks the aggregation funnel (i.e. the conformations stabilized by intermolecular interactions, indicated by the pink octagon); this portion of the energy landscape becomes inaccessible to the chain.

Folding mechanism and protein dynamics

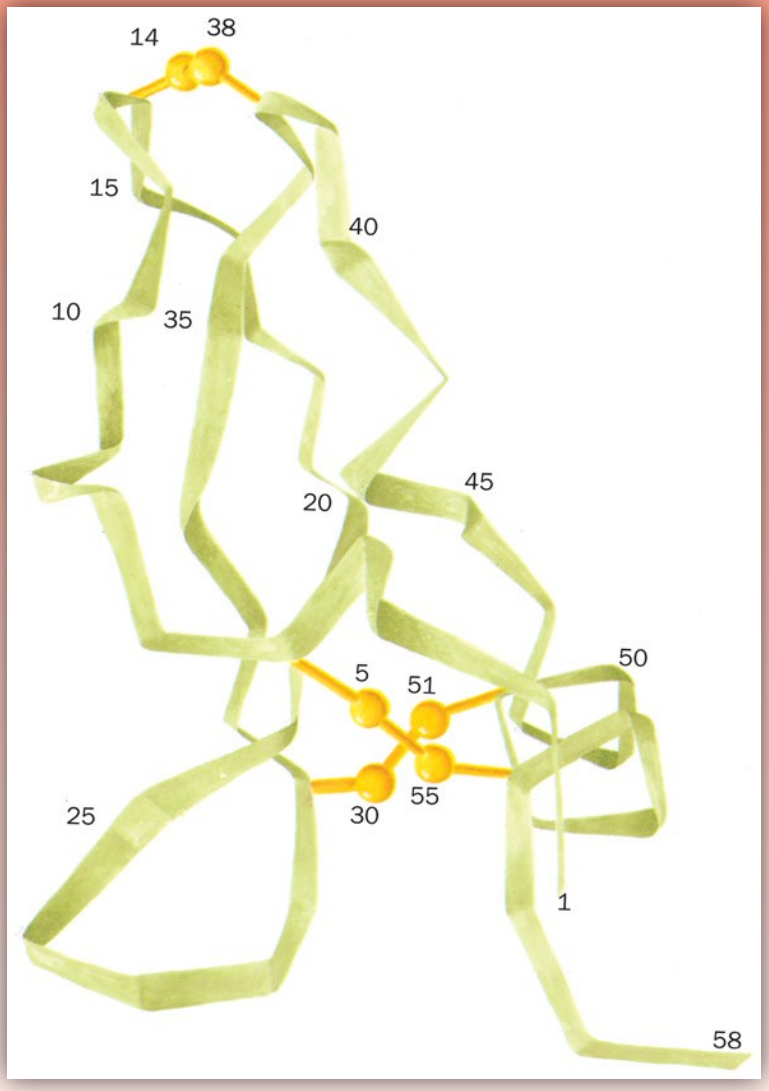

Folds via an ordered pathway: involves well defined intermediates

Polypeptide backbone and disulfide bonds of native BPTI (bovine pancreatic trypsin inhibitor) (58 residues, three disulfide bonds)

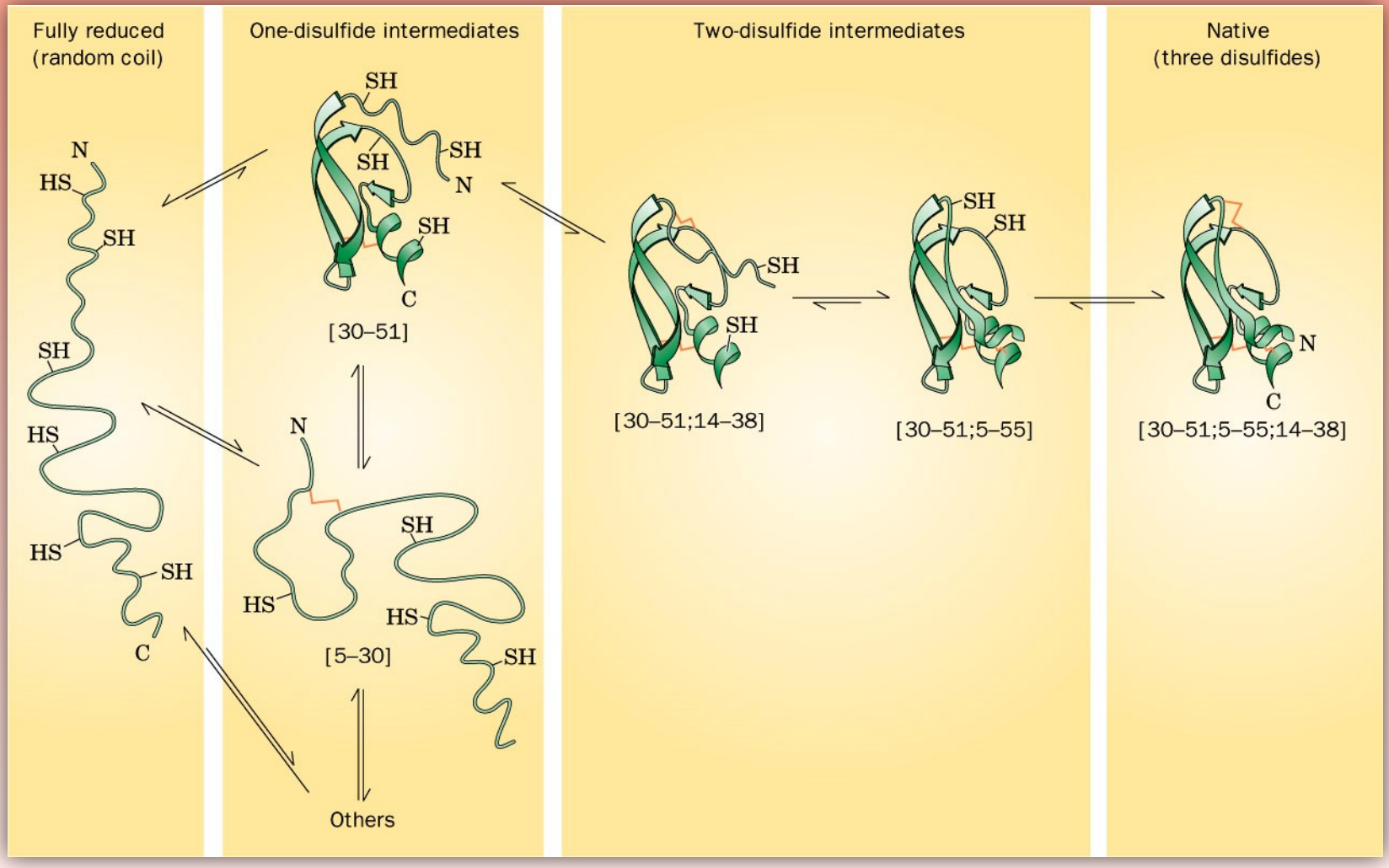

Renaturation of BPTI: protein primary structures evolved to specify efficient folding pathways as well as stable native conformations

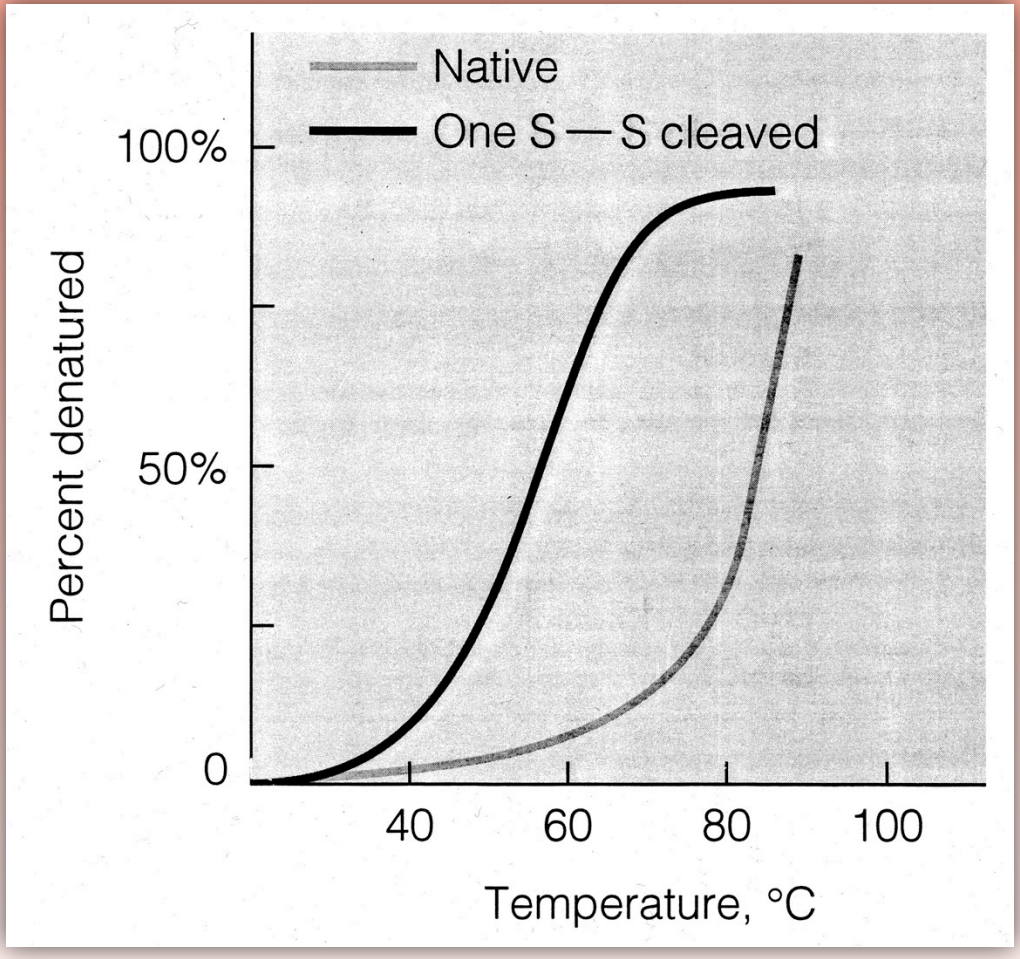

The effect of disulfide bonds on protein stability:
Reducing the number of disulfide bonds from 3 to 2 in BPTI reduces its T_m.

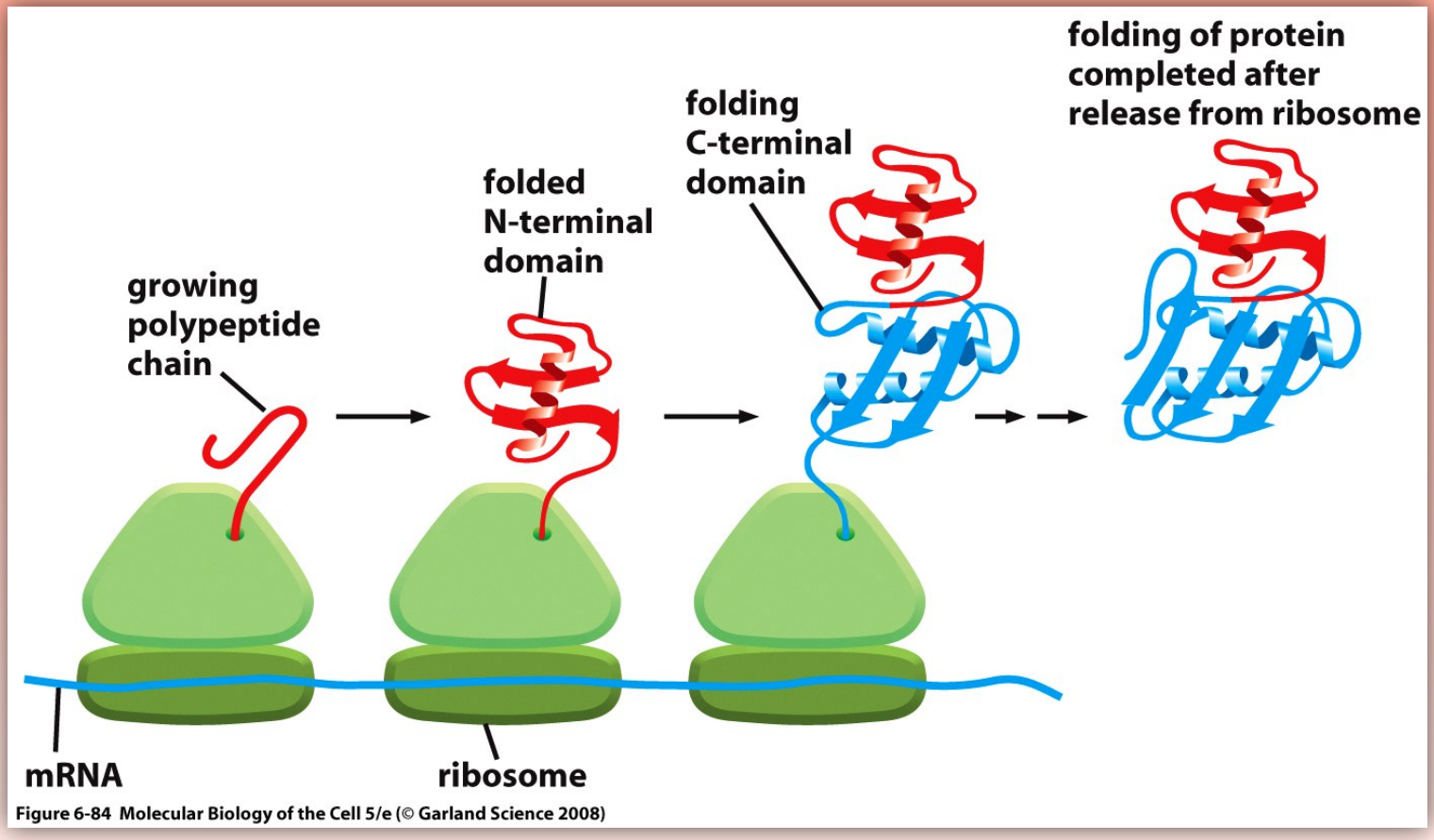

Figure 6-84 Molecular Biology of the Cell 5/e (© Garland Science 2008)

Co-translational protein folding: Sometimes the protein has not reached its native conformation when it is released from the ribosome.

Folding accessory proteins

a. protein disulfide isomerases (PDI)
b. peptidyl prolyl *cis-trans* isomerases
c. molecular chaperones

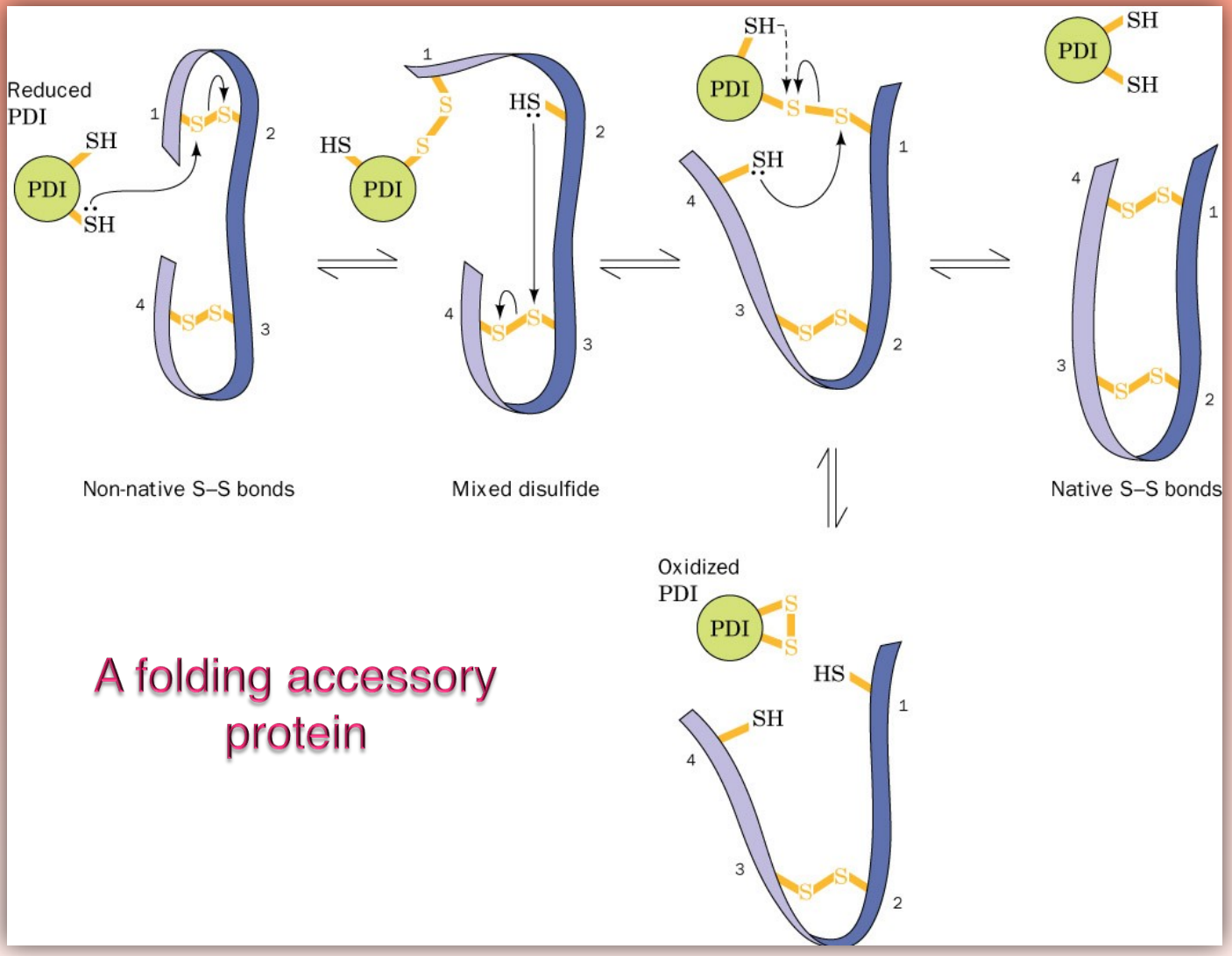

Reactions catalyzed by **protein disulfide isomerase** (PDI). The reduced PDI catalyzes the rearrangement of non-native disulfide bonds.

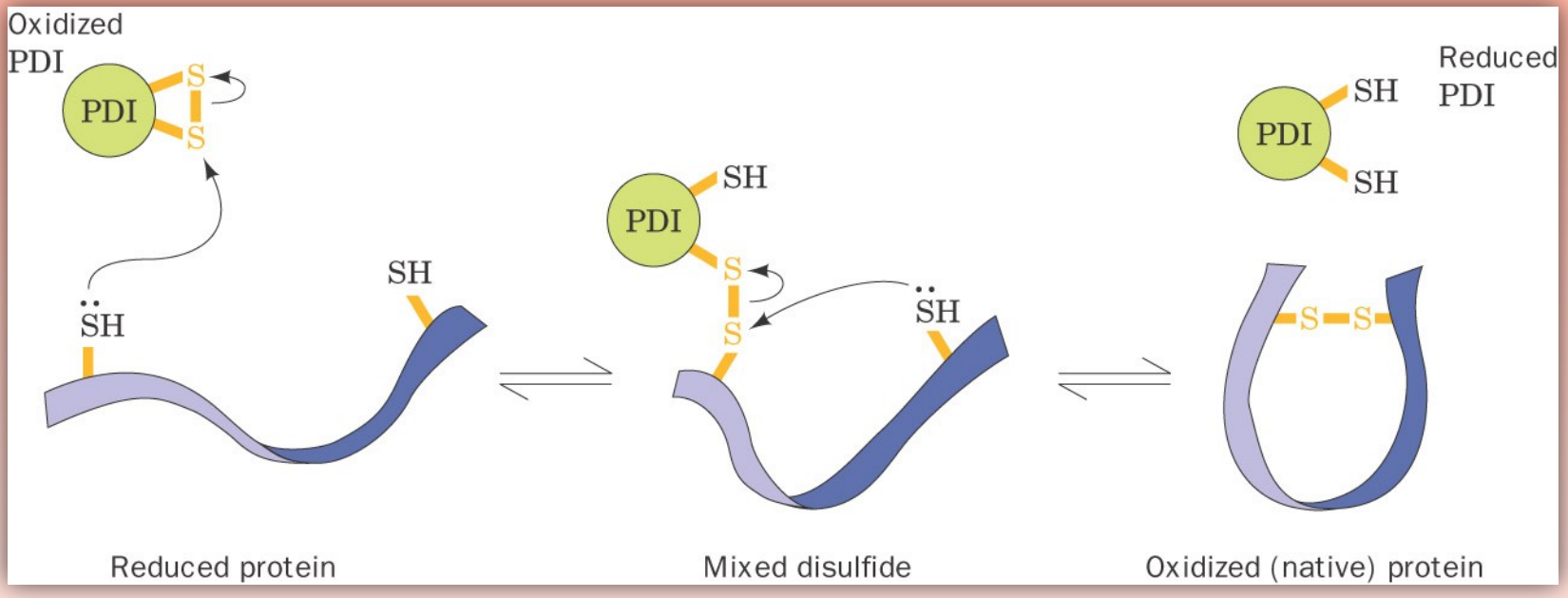

Reactions catalyzed by protein disulfide isomerase (PDI). The oxidized PDI-dependent synthesis of disulfide bonds in proteins.

Peptidyl Prolyl *Cis-Trans* Isomerases (PPIs)

Xaa-Pro peptide bonds: ~10% *cis*

PPIs catalyze the otherwise slow interconversion of Xaa-Pro peptide bonds between their *cis* and *trans* configurations; accelerate the folding of Pro-containing polypeptides.

Molecular Chaperones

Unfolded proteins *in vivo* have a great tendency to form intramolecular and intermolecular aggregates.

Molecular chaperones prevent/reverse improper associations, especially in multidomain and multisubunit proteins.

Function by binding solvent-exposed hydrophobic surfaces reversibly to promote proper folding

Many chaperones are ATPases.

Classes of Chaperones

A. Heat shock proteins 70: 70 kD monomeric proteins

B. Chaperonins: form large multisubunit cage-like assemblies

C. Hsp90: involved in signal transduction; very abundant in eukaryotes

D. Nucleoplasmins: acidic nuclear proteins involved in nucleosome assembly

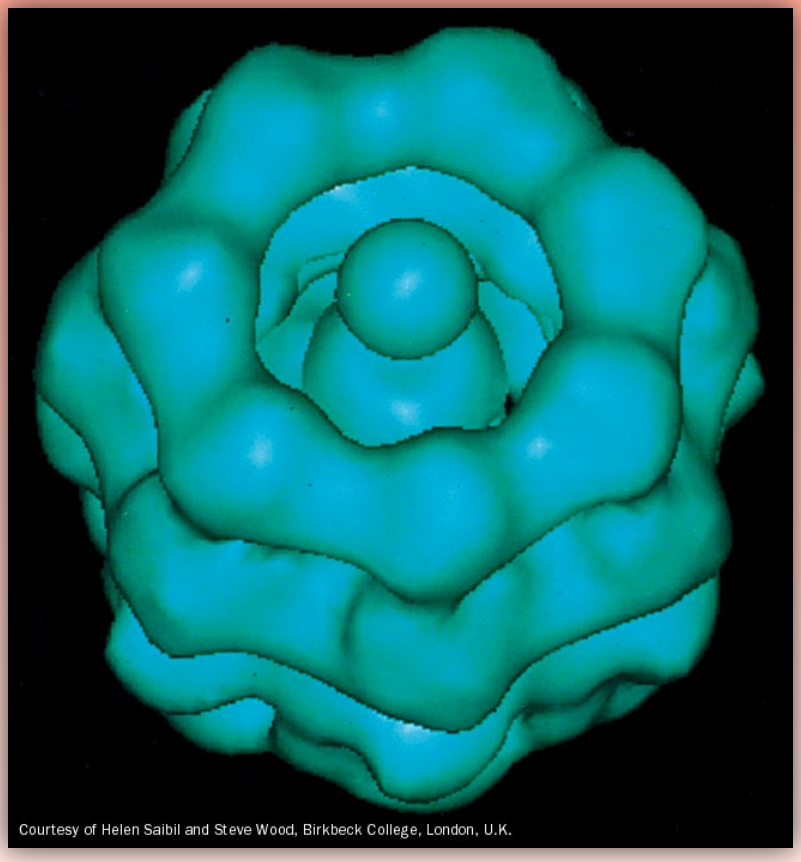

Chaperonins

GroEL/ES system (bacteria)

14 identical ~60 kD subunits in two rings; creates a central cavity

Electron micrograph-derived 3D image of the Hsp60 (GroEL) chaperonin from the photosynthetic bacterium *Rhodobacter sphaeroides*

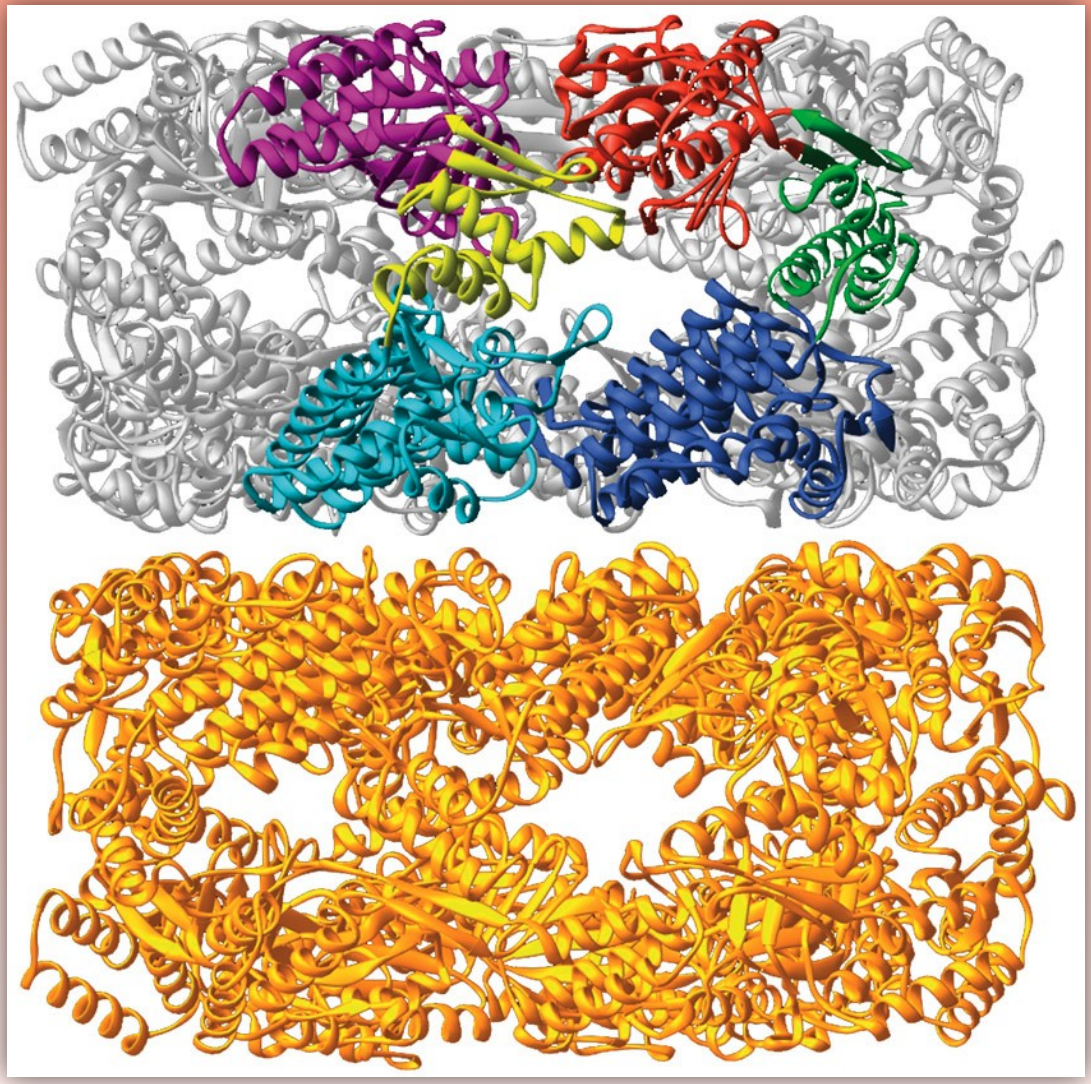

X-ray structure of GroEL. Side view perpendicular to the 7-fold axis

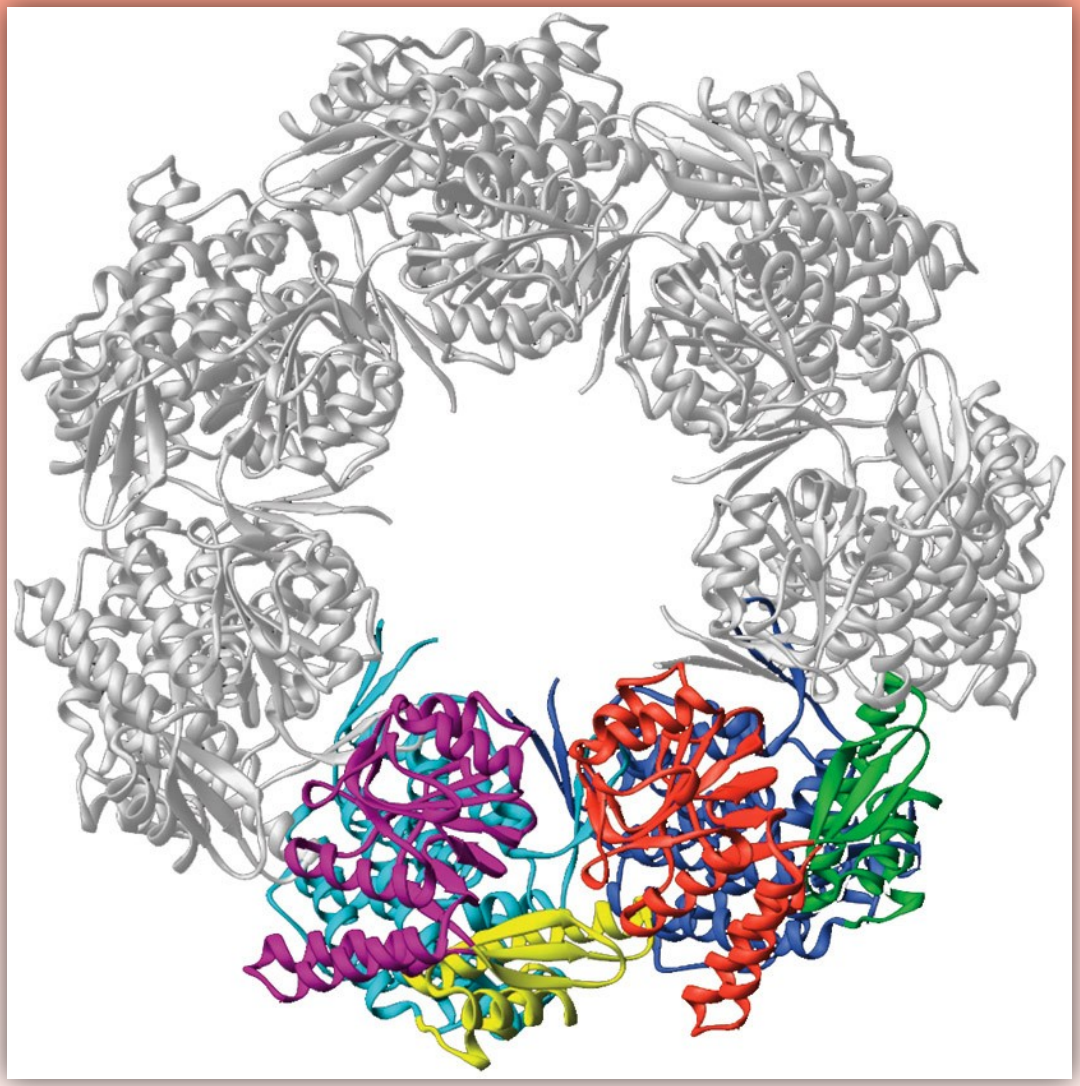

X-ray structure of GroEL. Top view along the 7-fold axis

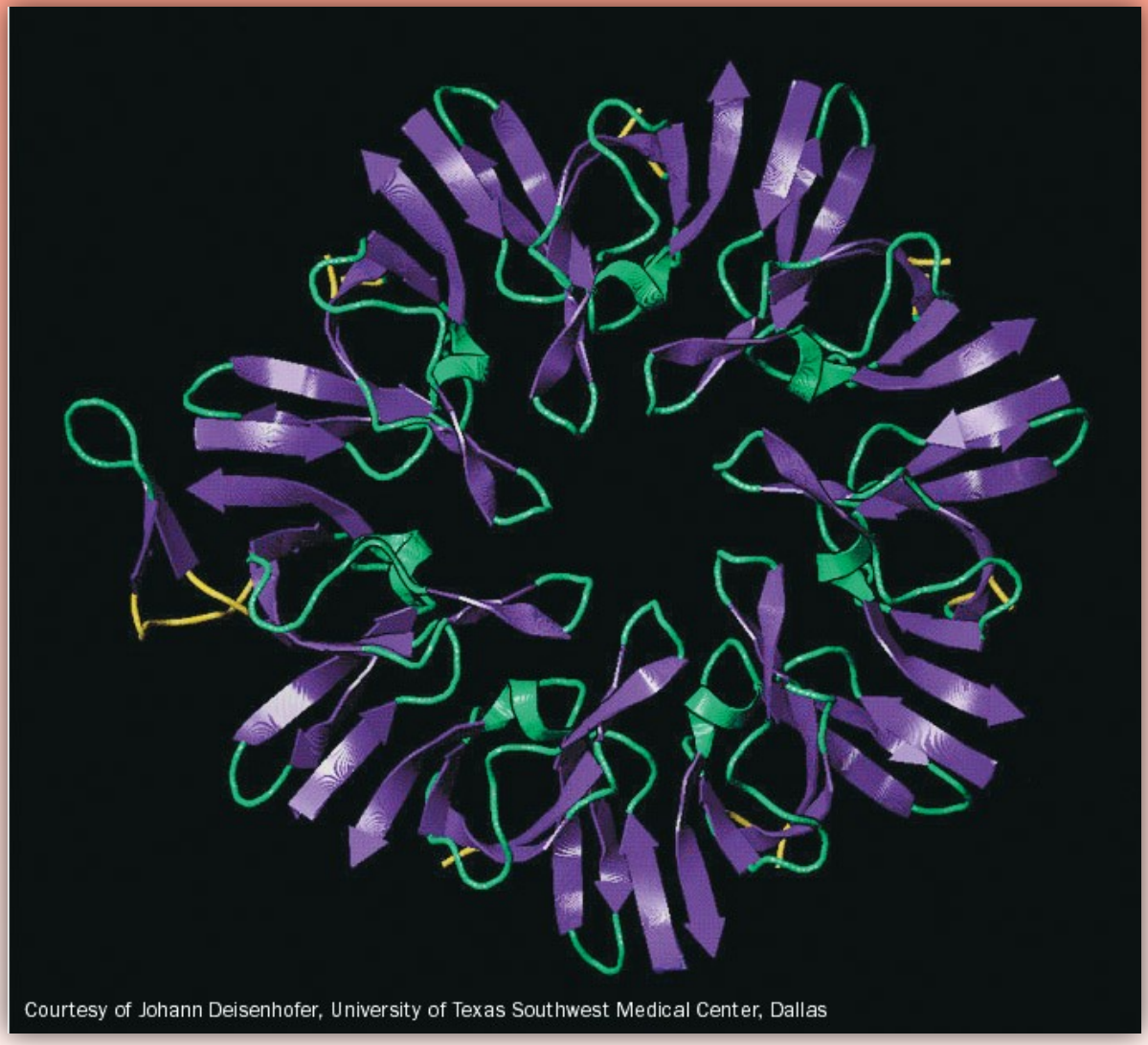

X-ray structure of GroES viewed along its 7-fold axis

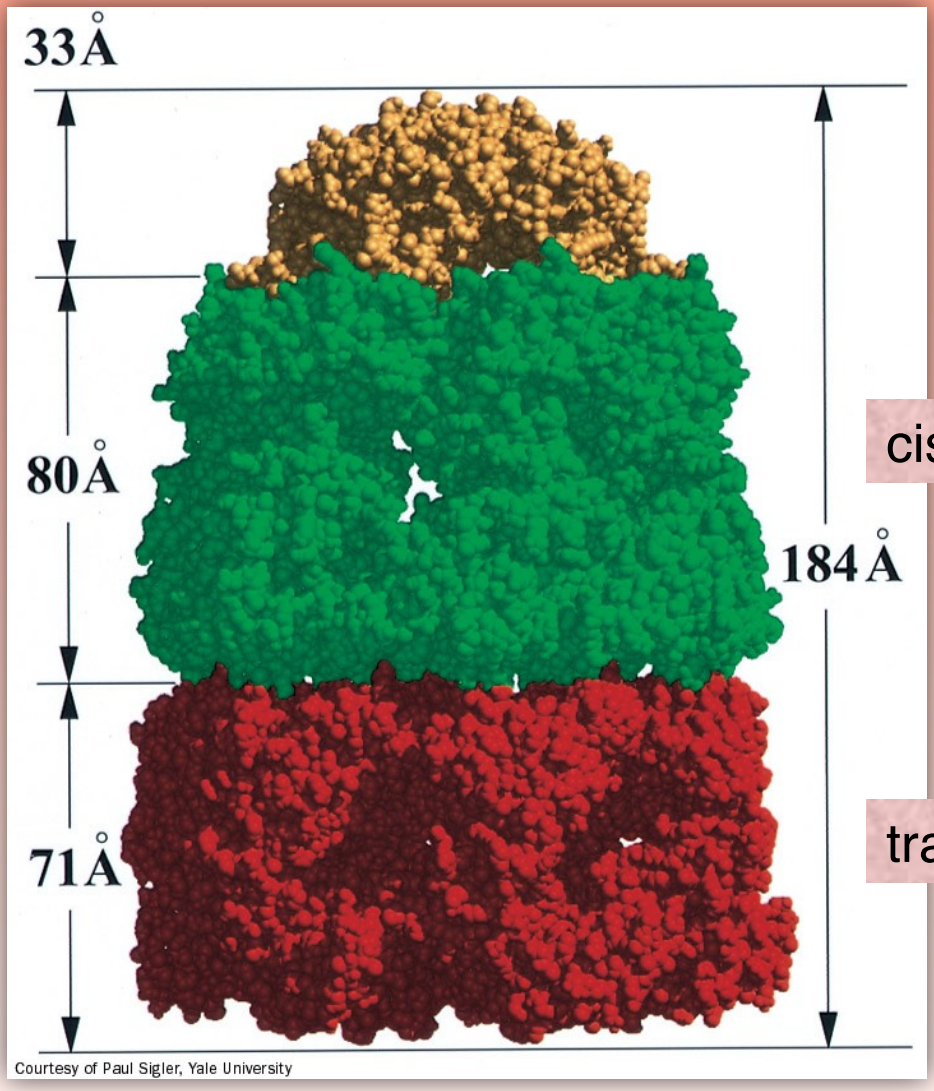

X-ray structure of the GroEL-GroES-$(ADP)_7$ complex. Side view

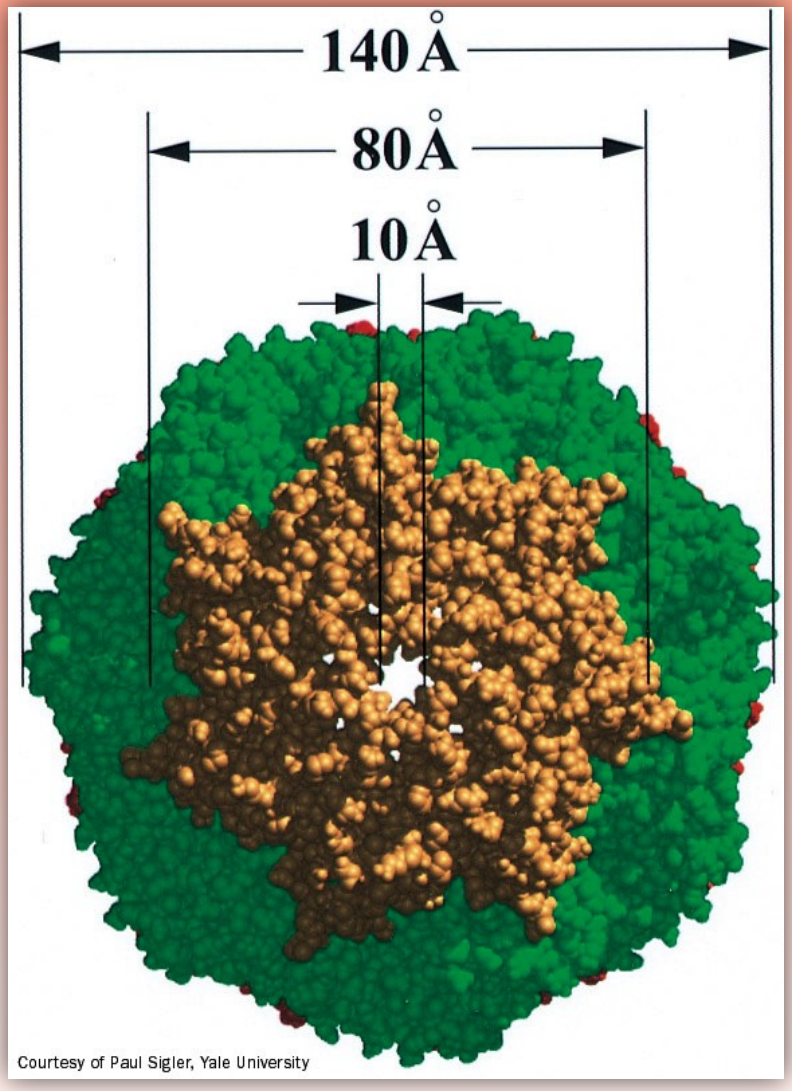

X-ray structure of the GroEL-GroES-$(ADP)_7$ complex.
Top view

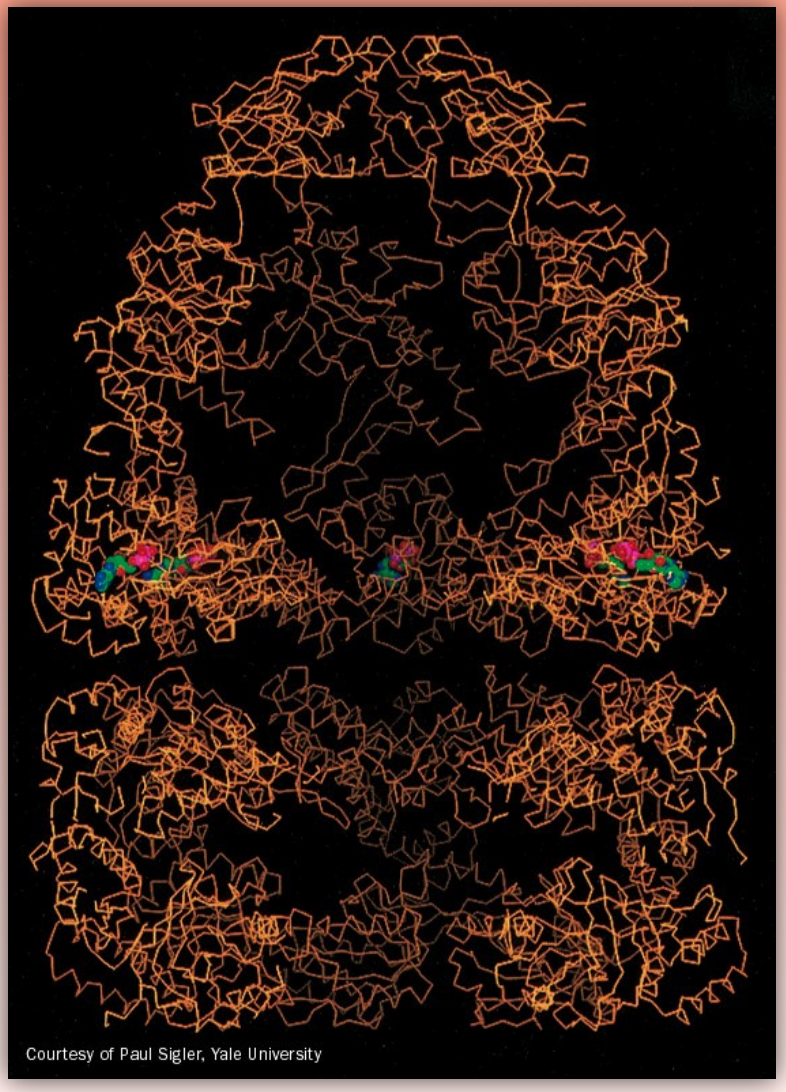

bound ADP shown
in cis ring

X-ray structure of the GroEL-GroES-$(ADP)_7$ complex

Subunits composed of three domains

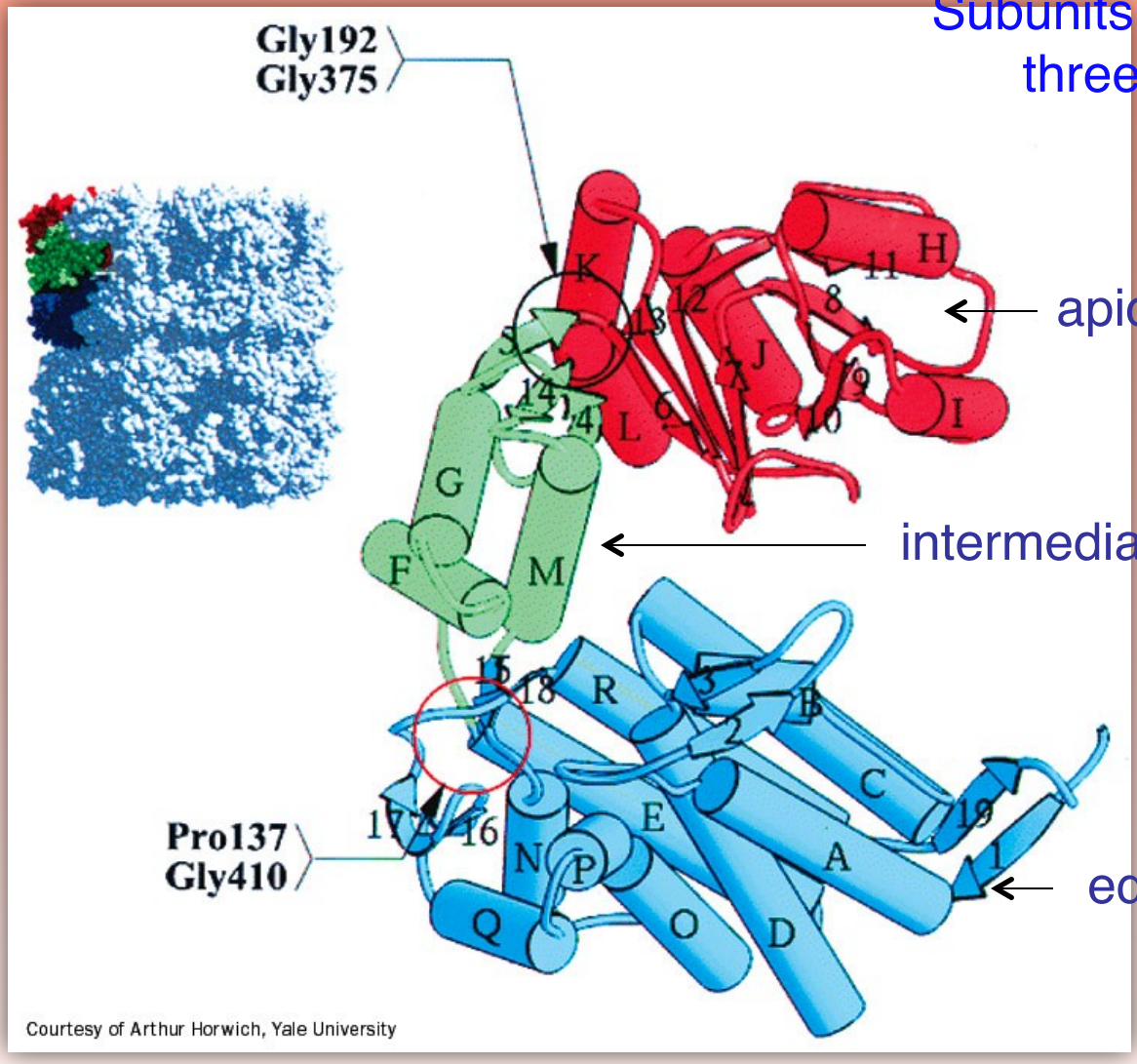

Domain movements in GroEL: Ribbon diagram of a single subunit of GroEL in the x-ray structure of GroEL alone.

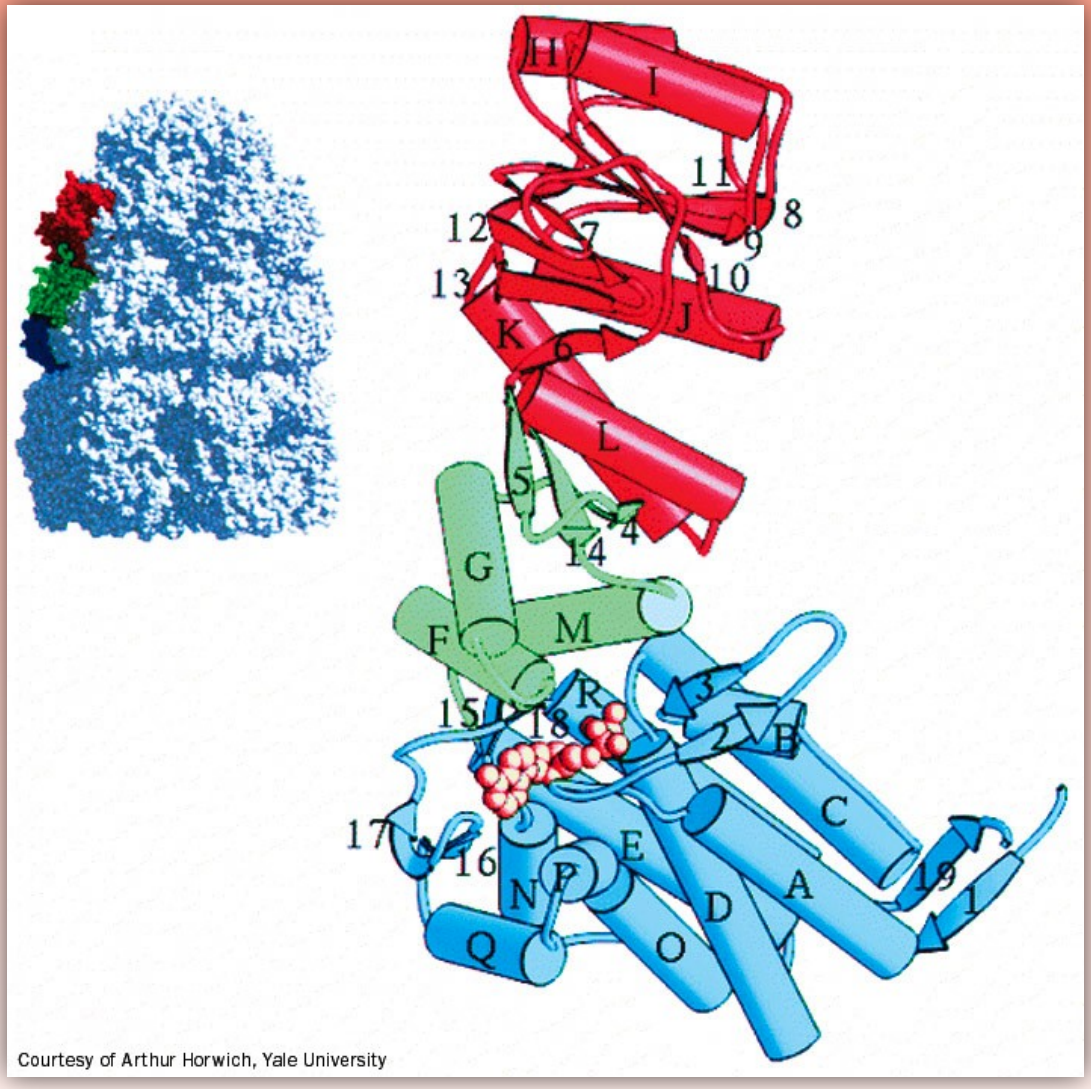

Domain movements in GroEL: A GroEL subunit in the x-ray structure of GroEL-GroES-$(ADP)_7$.

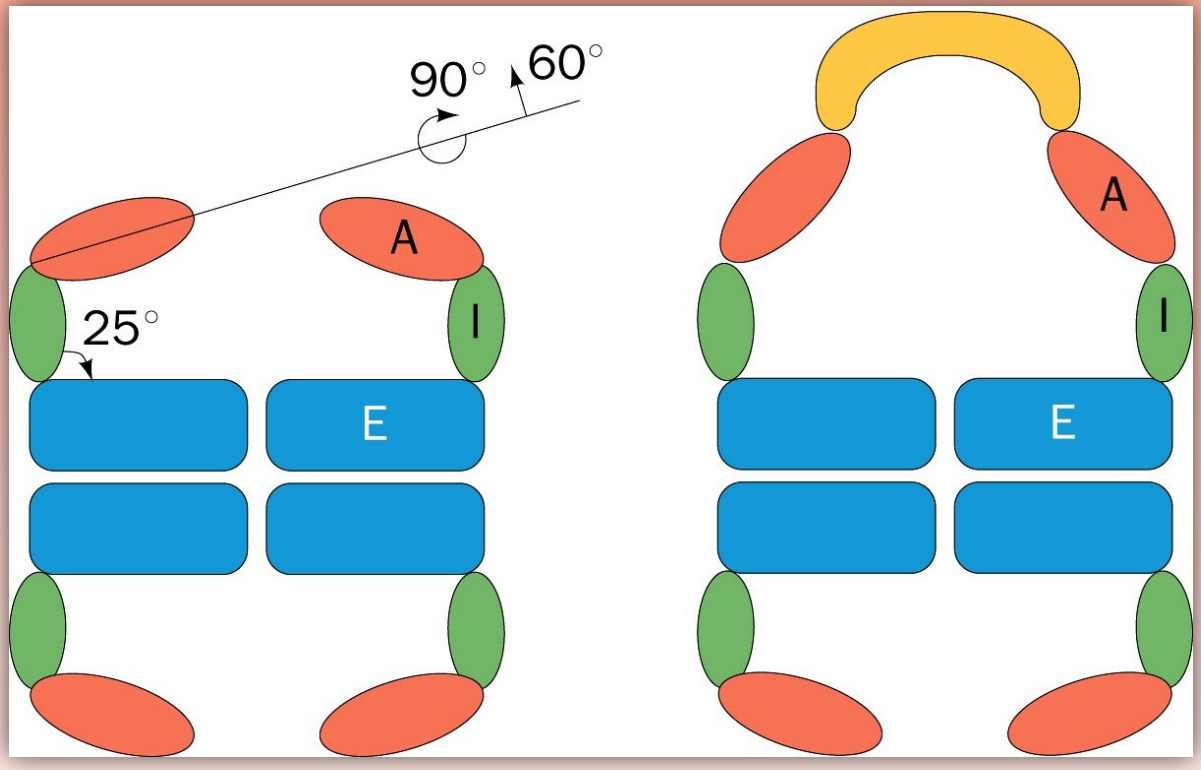

Domain movements in GroEL: Schematic diagram indicating the conformational changes in GroEL when it binds GroES.

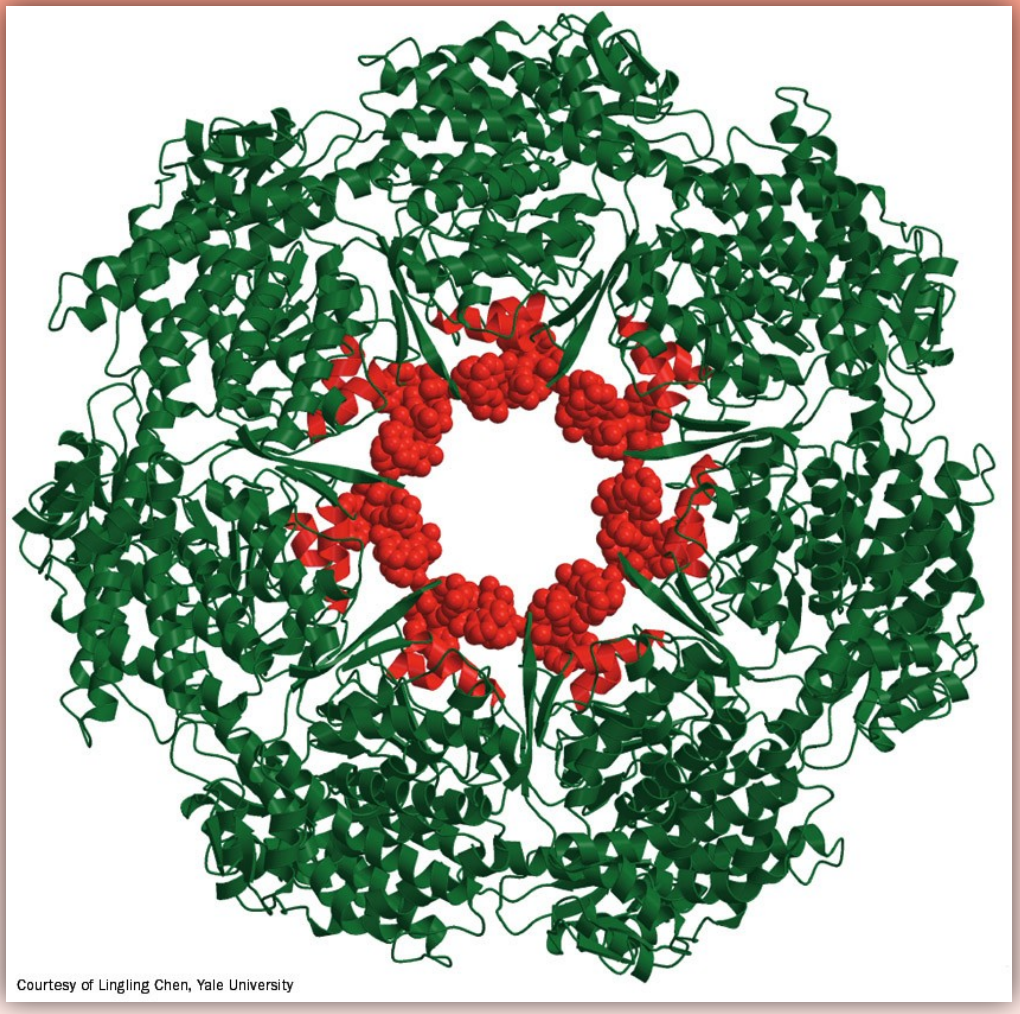

Apical domain of GroEL in complex with a tight-binding 12-residue polypeptide (SWMTTPWGFLHP) (hydrophobic residues indicated in blue)

GroEL alone

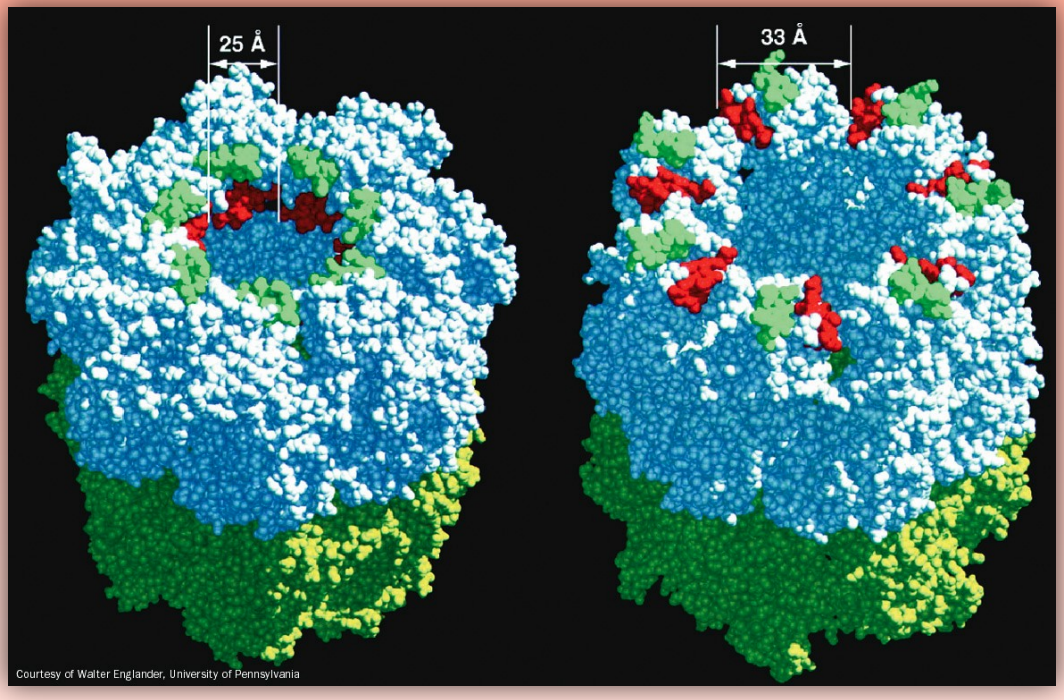

GroEL-GroES-$(ADP)_7$

(a) *(b)*

Hydrophobic binding sites on apical domains are green and red

Movements of the polypeptide-binding helices of GroEL

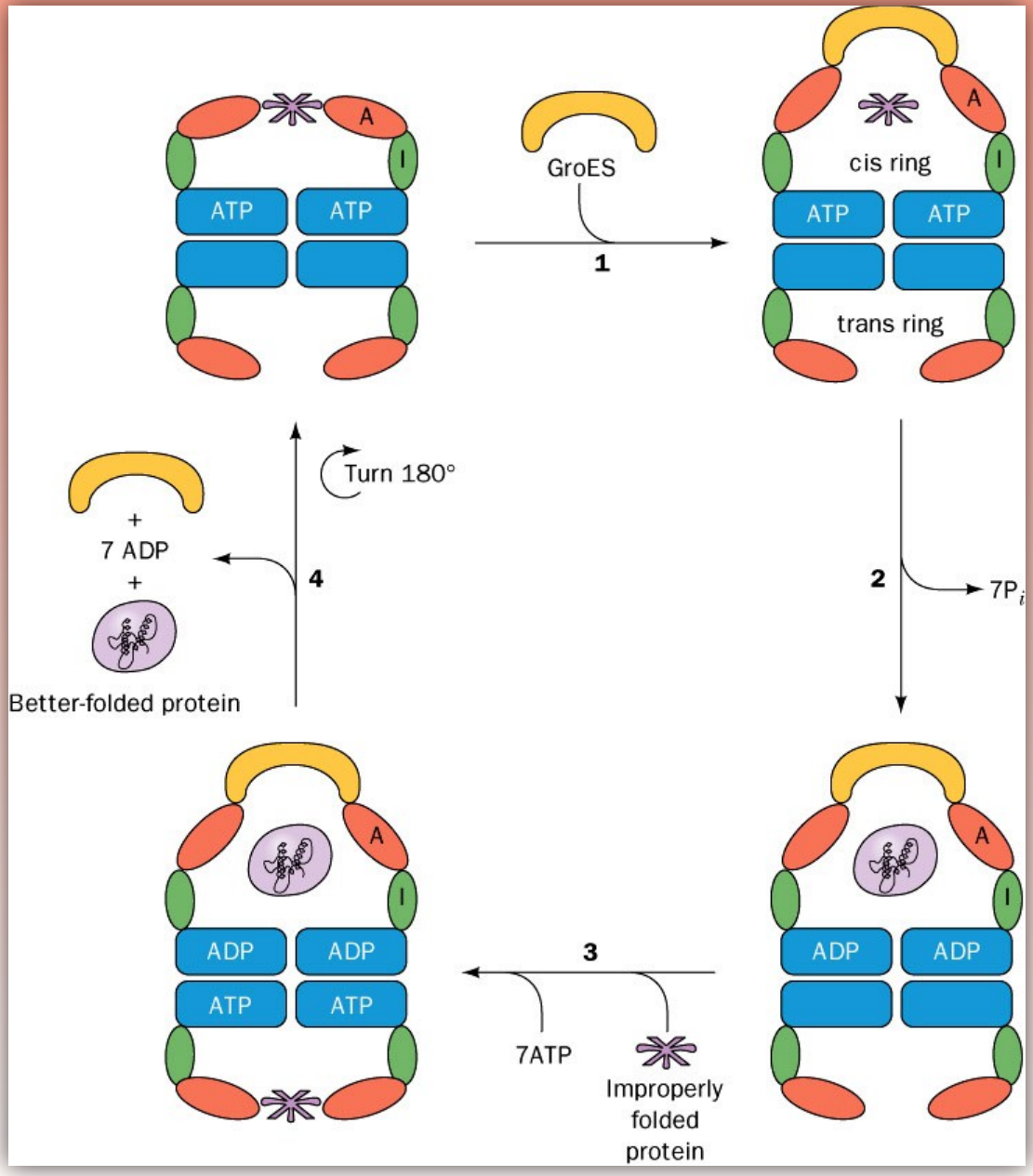

Reaction cycle of the GroEL/ES chaperonin system in protein folding

Models for GroEL/ES Action

A. Anfinsen cage model: folding within complex

B. Interative annealing: reversible release of partially folded intermediates (experimental evidence supports this model.

Protein dynamics

Proteins undergo structural motions that have functional significance.

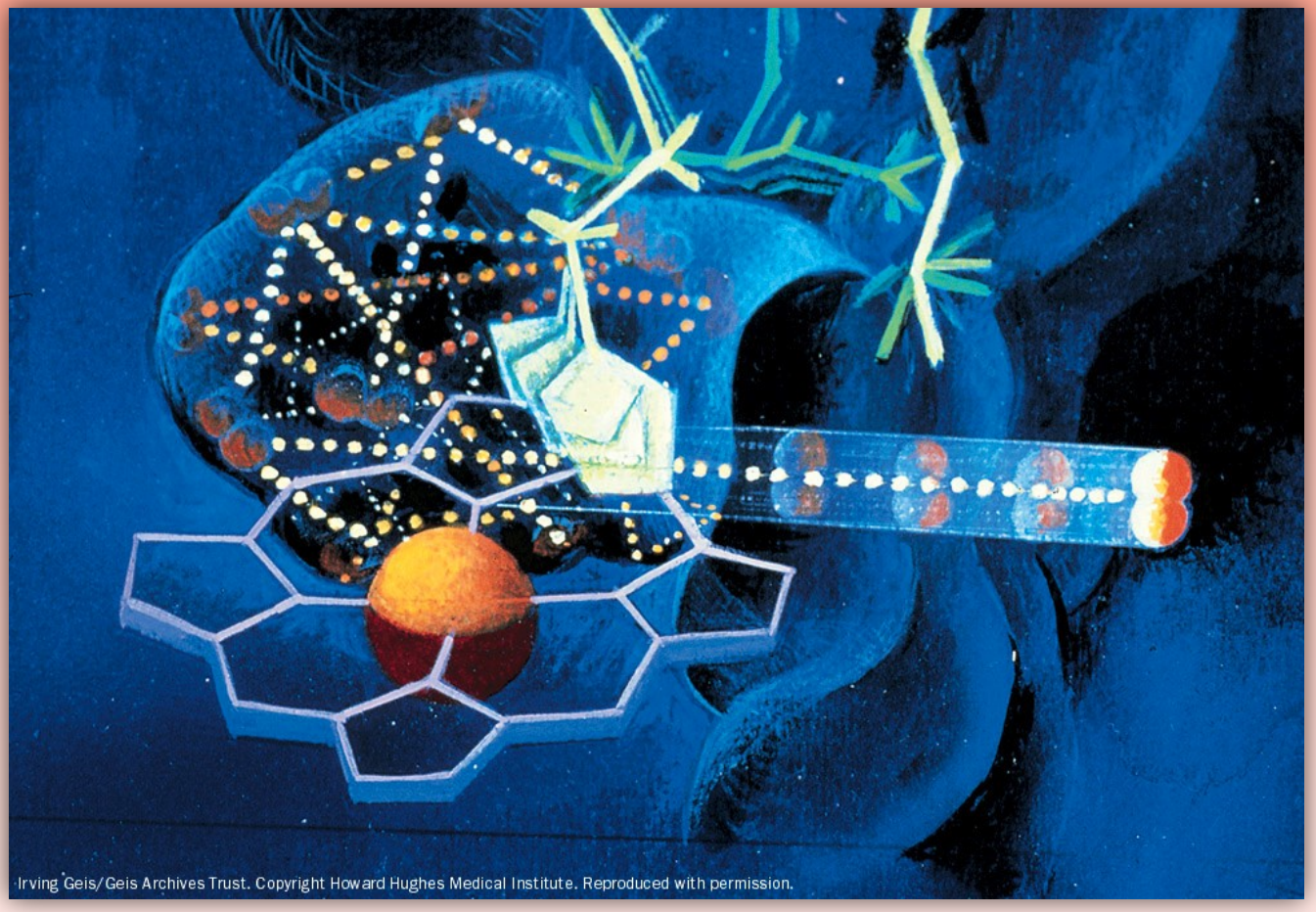

Conformational fluctuations (breathing motions) in the oxygen binding protein, myoglobin

Time-scales of protein motions

1. atomic fluctuations (10^{-15}-10^{-11} s; 0.01 - 1 Å displacements)
2. collective motions (10^{-12}-10^{-3} s; 0.01 - 5 Å displacements)
3. triggered conformational changes (10^{-9} -10^{3} s; 0.5 - 10 Å displacements)

Techniques: crystallography, NMR, molecular dynamics (MD) simulations

The internal motions of myoglobin as determined by a molecular dynamics (MD) simulation: the C_α backbone and the heme group

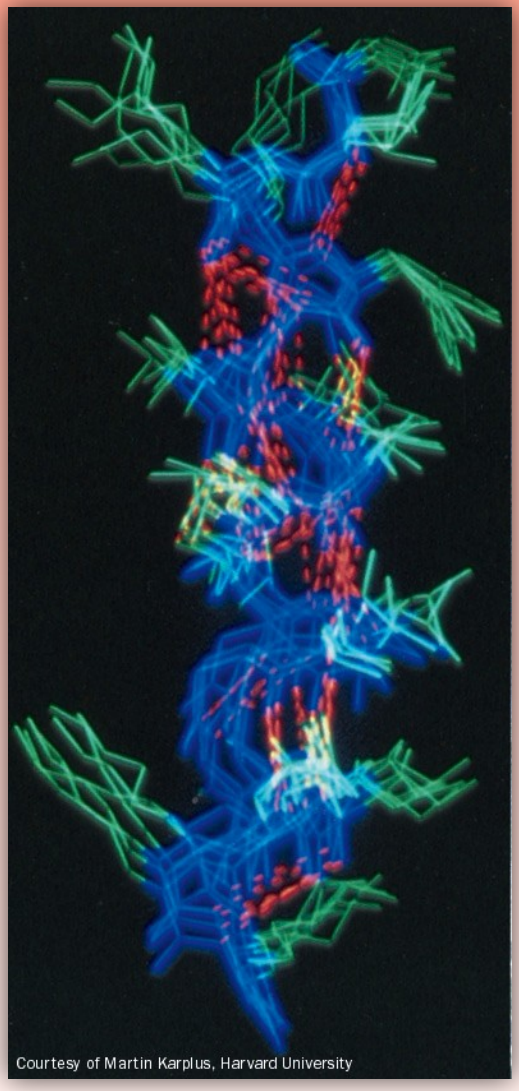

The internal motions of myoglobin as determined by a molecular dynamics (MD) simulation: an α helix

Conformational Diseases: Amyloid and Prions

Alzheimer and Huntington diseases;
transmissible spongiform
encephalopathies (TSEs);
amyloidoses

Common characteristic: formation of amyloid fibrils

The involved proteins assume two different
stable conformations (native and amyloid)

Table 6-4 Some Protein Misfolding Diseases

Disease	Defective Protein
Alzheimer's disease	Amyloid-β protein
Amyotrophic lateral sclerosis	Superoxide dismutase
Huntington's disease	Huntingtin with polyglutamate expansion
Lysozyme amyloidosis	Lysozyme
Hereditary renal amyloidosis	Fibrinogen
Parkinson's disease	α-Synuclein
Transmissible spongiform encephalopathies (TSEs)	Prion protein

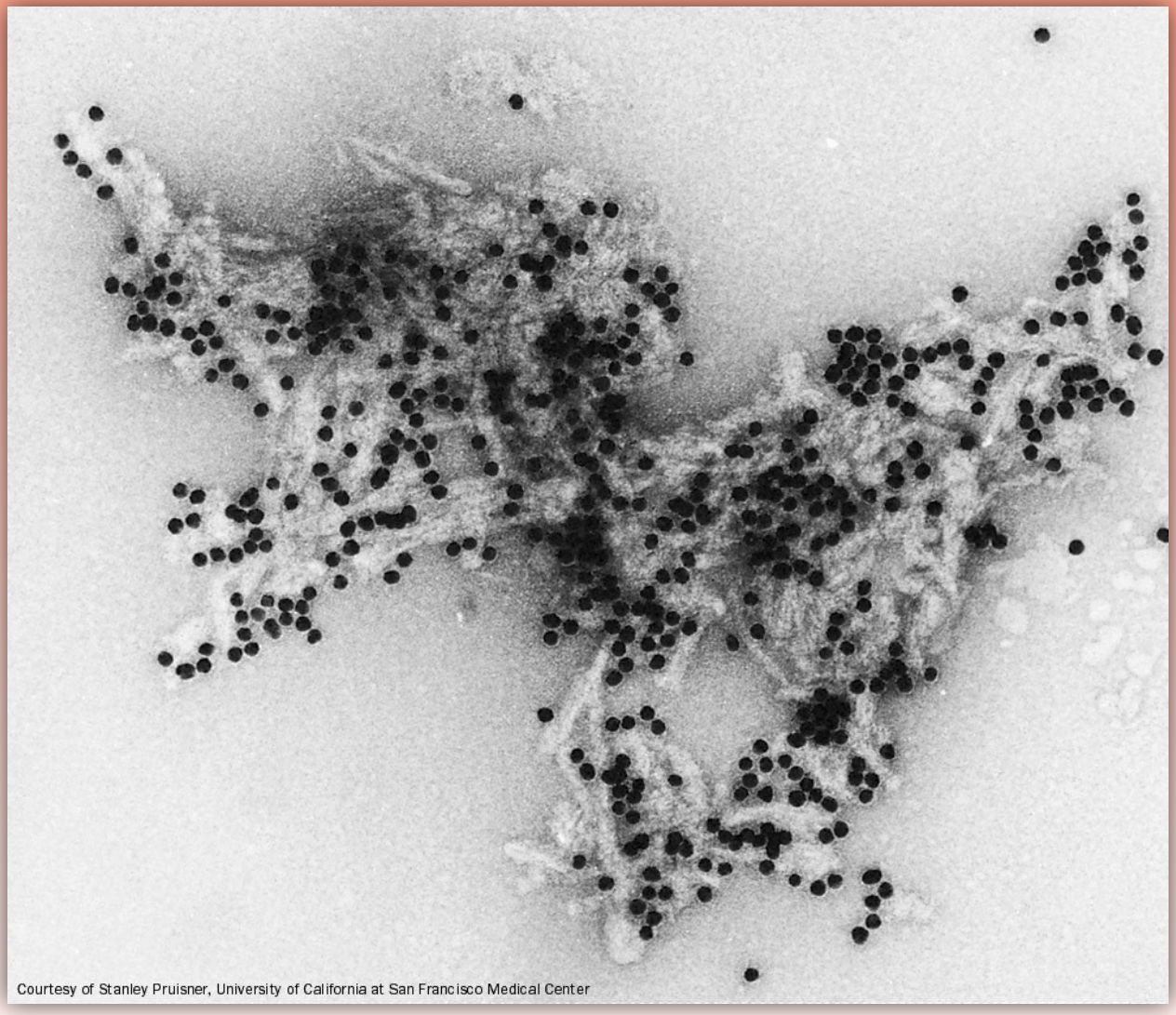

Amyloid fibrils: an electron micrograph of amyloid fibrils of the protein PrP 27-30.

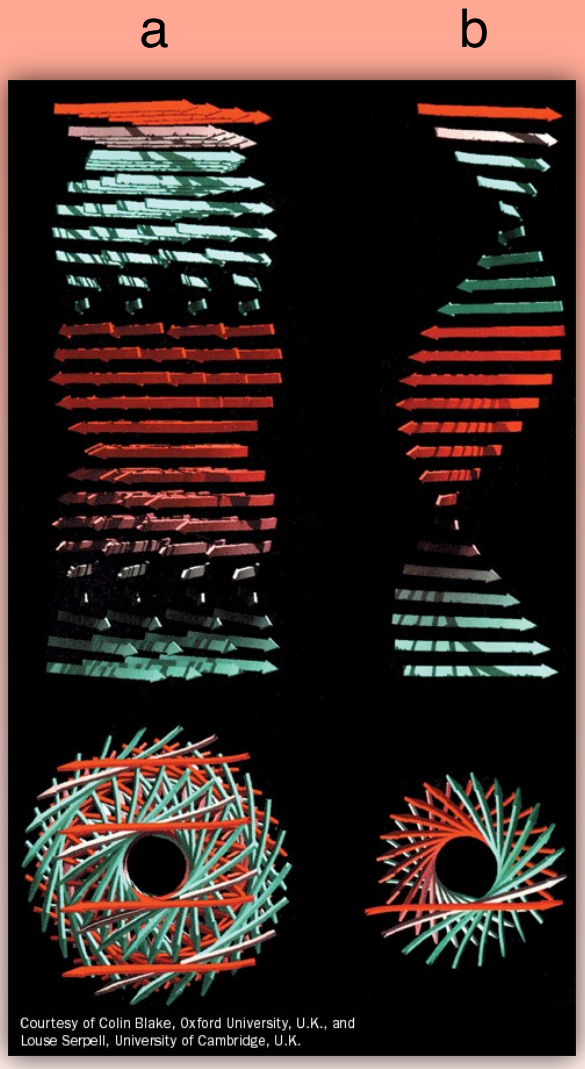

Fibrils consist mainly of β-sheets whose β-strands are perpendicular to the fibril axis.

Amyloid fibrils (PrP 27-30): Full model (a) and isolated β sheet (b).

Amyloidogenic proteins are mutant forms of normally occurring proteins.

Lysozyme mutants occur in familial visceral amyloidosis.

Superposition of wild-type human lysozyme and its D67H mutant.

Prion diseases can be spread from one organism to another

transmissible spongiform encephalopathies (TCEs)
(scrapie; mad cow or BSE; Creutzfeldt-Jakob disease)

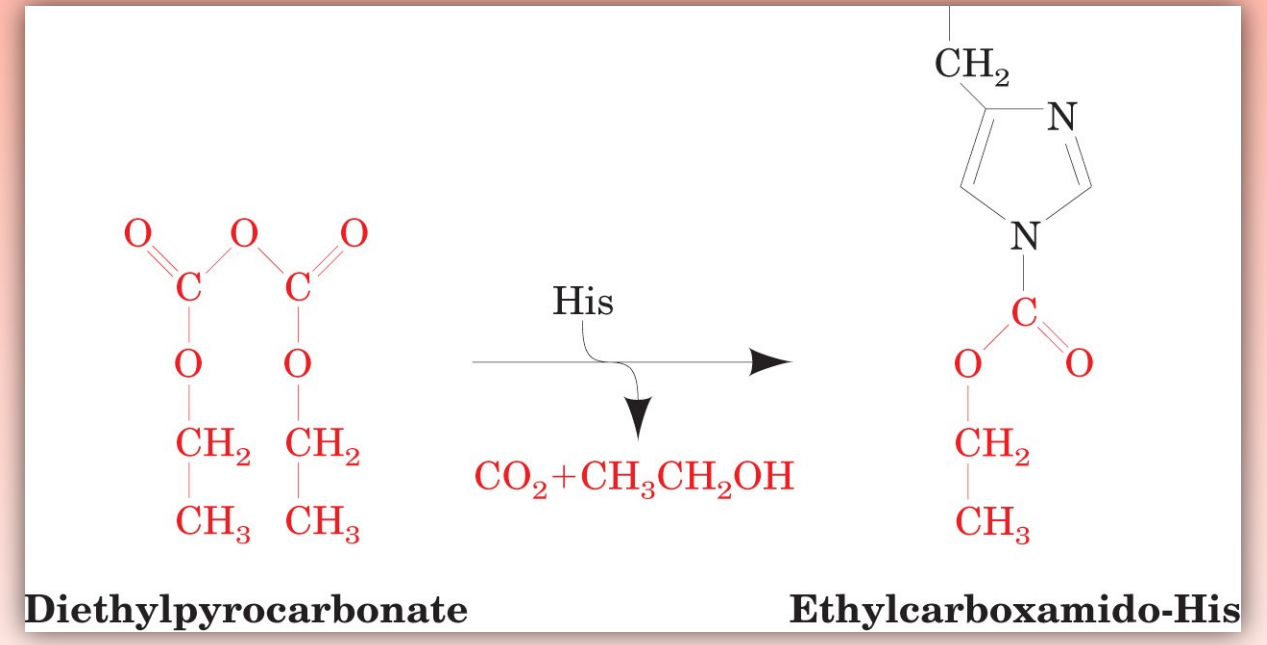

Evidence that the scrapie agent is a protein: scrapie agent is inactivated by treatment with diethylpyrocarbonate, which reacts with histidine sidechains.

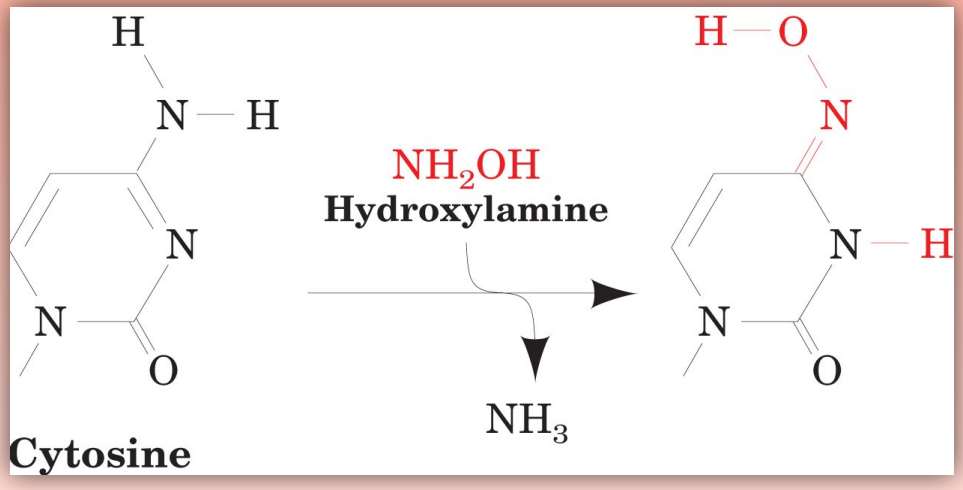

Evidence that the scrapie agent is a protein:
scrapie agent is unaffected by treatment with hydroxylamine, which reacts with cytosine residues.

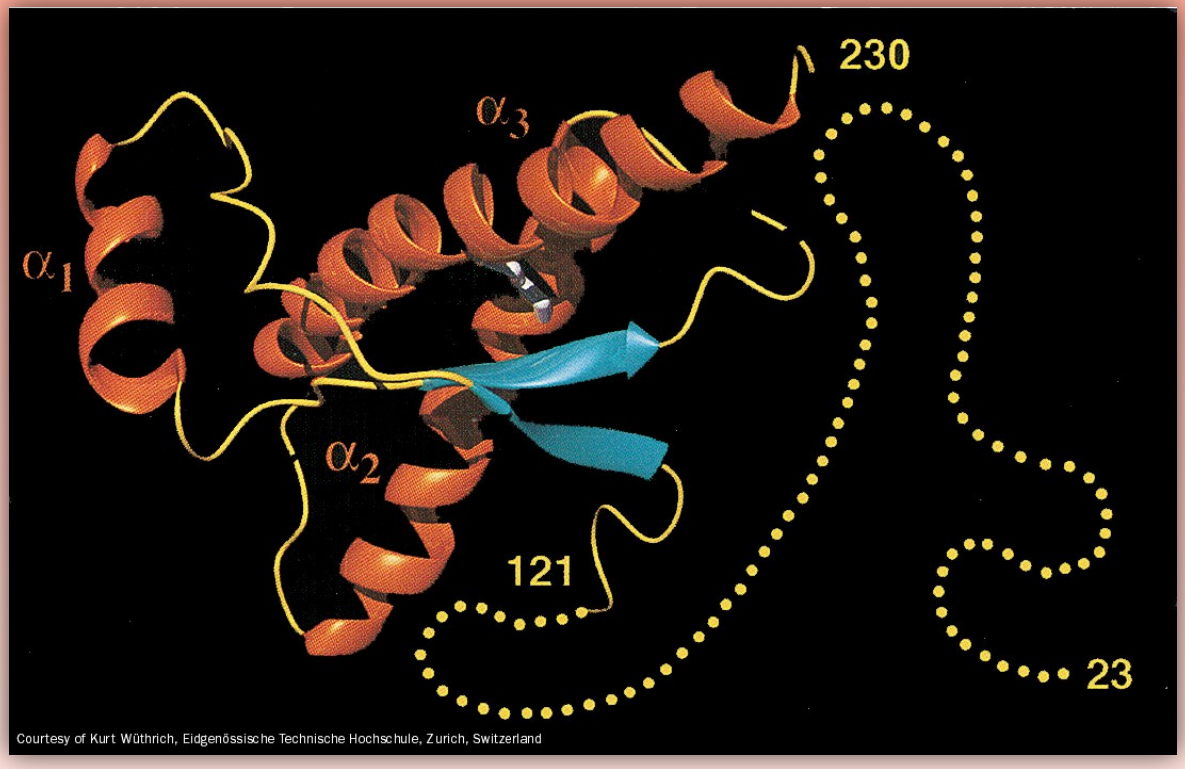

Prion protein conformations: NMR structure of human prion protein (PrP^C). Note the disordered *N*-terminal tail residues (dots). PrP may be a cell-surface signal receptor.

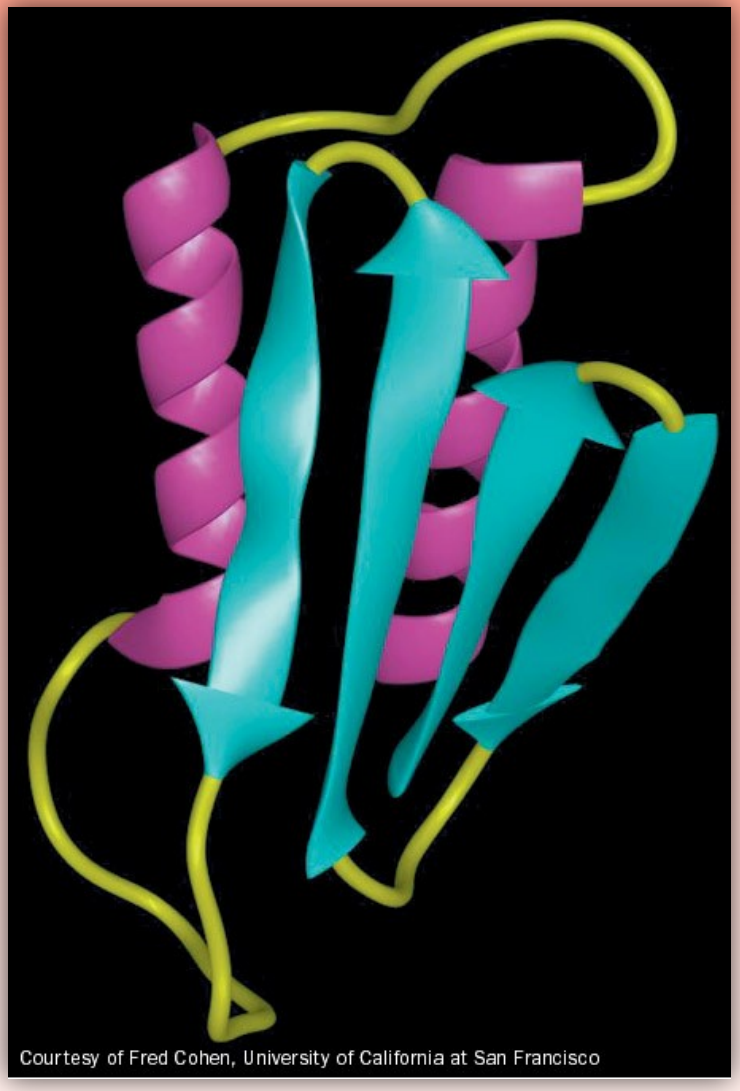

Prion hypothesis: PrP^{Sc} induces the conversion of PrP^{C} to Prp^{Sc}

Conversion may be mediated by a molecular chaperone.

Prion protein conformations: a plausible model for the structure of PrP^{Sc} (very insoluble)

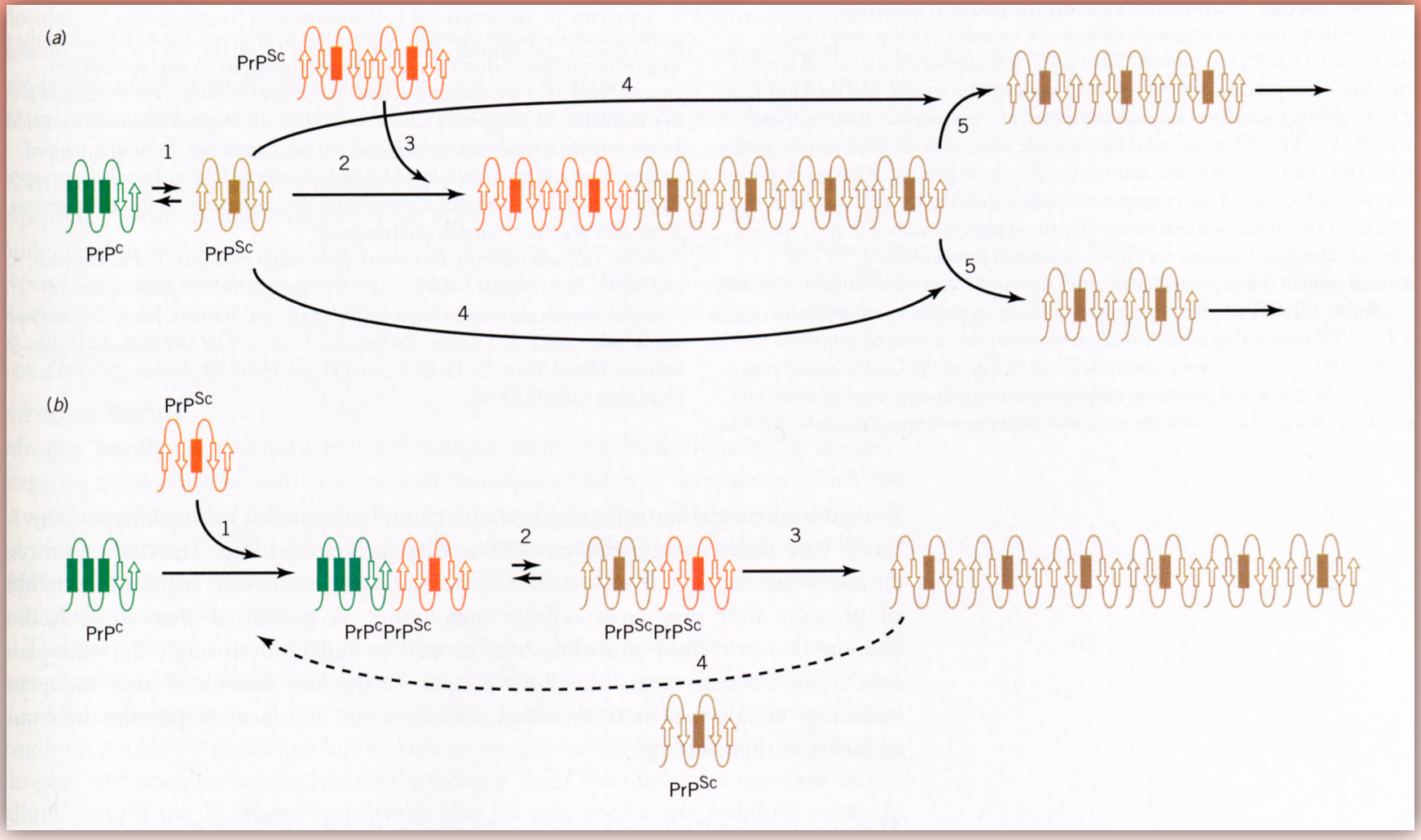

Mechanisms of amyloid plaque formation: (a) The nucleation-polymerization mechanism. (b) The template-directed mechanism.